



HAL
open science

Analysis of a simplified model of the urine concentration mechanism

Magali Tournus, Aurélie Edwards, Nicolas Seguin, Benoît Perthame

► To cite this version:

Magali Tournus, Aurélie Edwards, Nicolas Seguin, Benoît Perthame. Analysis of a simplified model of the urine concentration mechanism. *Networks and Heterogeneous Media*, 2012, 7 (4), pp.989-1018. 10.3934/nhm.2012.7.989 . hal-00605109v2

HAL Id: hal-00605109

<https://hal.science/hal-00605109v2>

Submitted on 3 Mar 2013

HAL is a multi-disciplinary open access archive for the deposit and dissemination of scientific research documents, whether they are published or not. The documents may come from teaching and research institutions in France or abroad, or from public or private research centers.

L'archive ouverte pluridisciplinaire **HAL**, est destinée au dépôt et à la diffusion de documents scientifiques de niveau recherche, publiés ou non, émanant des établissements d'enseignement et de recherche français ou étrangers, des laboratoires publics ou privés.

ANALYSIS OF A SIMPLIFIED MODEL OF THE URINE CONCENTRATION MECHANISM

MAGALI TOURNUS

UPMC Univ Paris 06, UMR 7598, Laboratoire Jacques-Louis Lions
F-75005, Paris, France
CNRS, UMR 7598, Laboratoire Jacques-Louis Lions
F-75005, Paris, France
Univ Paris 05, INSERM UMRS872, and CNRS ERL7226,
Laboratoire de génomique, physiologie et physiopathologie rénales
Centre de Recherche des Cordeliers, 75006, Paris, France

AURÉLIE EDWARDS

Univ Paris 06, Univ Paris 05, INSERM UMRS 872, and CNRS ERL 7226
Laboratoire de génomique, physiologie et physiopathologie rénales
Centre de Recherche des Cordeliers, 75006, Paris, France

NICOLAS SEGUIN

UPMC Univ Paris 06, UMR 7598, Laboratoire Jacques-Louis Lions
F-75005, Paris, France
CNRS, UMR 7598, Laboratoire Jacques-Louis Lions
F-75005, Paris, France

BENOÎT PERTHAME

UPMC Univ Paris 06, UMR 7598, Laboratoire Jacques-Louis Lions
F-75005, Paris, France
CNRS, UMR 7598, Laboratoire Jacques-Louis Lions
F-75005, Paris, France
INRIA Paris-Rocquencourt, EPI BANG and Institut Universitaire de France

ABSTRACT. We study a nonlinear stationary system of transport equations with specific boundary conditions describing the transport of solutes dissolved in a fluid circulating in a countercurrent tubular architecture, which constitutes a simplified model of a kidney nephron. We prove that for every Lipschitz and monotonic nonlinearity (which stems from active transport across the ascending limb), the dynamic system, a PDE which we study through contraction properties, relaxes toward the unique stationary state. A study of the linearized stationary operator enables us, using eigenelements, to further show that under certain conditions regarding the nonlinearity, the relaxation is exponential. We also describe a finite volume scheme which allows us to efficiently approach the numerical solution to the stationary system. Finally, we apply this numerical method to illustrate how the countercurrent arrangement of tubes enhances the axial concentration gradient, thereby favoring the production of highly concentrated urine.

2000 *Mathematics Subject Classification.* 35L60, 92C35, 34B45.

Key words and phrases. Countercurrent, nonlinear transport equation, solute transport, relaxation toward steady state, contraction property.

1. Introduction. The main role of the kidney is to maintain fluid and electrolyte homeostasis, by regulating the volume and composition of blood so that it remains clean and chemically balanced. Kidneys receive blood from the renal artery, filter it, and return it to the body via the renal vein while excreting unwanted substances in the urine. The functional units of the kidney, known as nephrons, each consist of several segments arranged in a countercurrent manner so as to maximize the production of concentrated urine. A countercurrent system is composed of two juxtaposed branches, such that fluid in one branch flows in the opposite direction as fluid in the other branch. In a cocurrent system, by contrast, fluid flows in the same direction in both branches. The importance of countercurrent exchange for the urine concentrating mechanism has been recognized since the 1950s [20].

Our purpose is to develop a simplified mathematical model predicated on a steady state model describing solute transport in nephrons, to prove that the solution to the dynamic model we defined relaxes toward the solution to the steady state model, and to compute this solution. In this simplified representation, the nephron consists of 3 water-impermeable tubes that exchange solutes via a common interstitium, as illustrated in Figure 1. There have been other simplified models of renal function based on similar hypotheses [5].

More sophisticated models have been built since, in particular by Layton & Layton and colleagues. The ENO (essentially non-oscillatory) methodology, an explicit method, was used to obtain dynamic and steady-state solutions [10] [13]. Due to stiffness, the time step had to be very small, resulting in high computational costs. An alternative, a semi-Lagrangian semi-implicit (SLSI) method was subsequently developed [9]. To improve accuracy, the method was combined with a Newton-type solver. In every instance, the purpose was to approach the stationary state. What makes our work novel is the formal demonstration that the dynamic system relaxes toward the stationary state, and that the latter is unique.

Here, we only consider one generic uncharged solute (e.g., NaCl), whose transport across walls is driven by diffusion and active pumps (which require metabolic energy to carry the solute against its concentration gradient). If the tubes were permeable to water, convection would also contribute to solute transport. In other words, by assuming that there is no water movement across the walls, we are neglecting the convective part of the solute flux. However, the latter is negligible in most renal tubules.

Models that account for the presence of blood vessels usually consider at least 5 tubes (i.e., tubules and vessels). We choose to only represent 3 here so as to keep the presentation and analysis tractable, but the problem formulation and the mathematical methods described herein apply to any number ≥ 3 .

Given the solute concentration (denoted C) at the inlet of tubes 1 and 2, and knowing that $C^3(L) = C^2(L)$ by continuity, our objective is to determine concentration profiles in the three tubes, as well as in the surrounding interstitium.

In each tube i , the fluid (mostly water) is assumed to flow at a constant rate. We define Q^i as the water flow rate in tube i , J^i as the transmural flux from the interstitium into tube i , and C_0^1 and C_0^2 are two given nonnegative values. At steady state, conservation of solute in each tube can be expressed as

$$\begin{cases} Q^1 \frac{dC^1(x)}{dx} = J^1(x), & x \in [0, L], \\ Q^2 \frac{dC^2(x)}{dx} = J^2(x), & x \in [0, L], \\ Q^3 \frac{dC^3(x)}{dx} = J^3(x), & x \in [0, L], \\ C^1(0) = C_0^1, & C^2(0) = C_0^2, & C^3(L) = C^2(L). \end{cases} \quad (1)$$

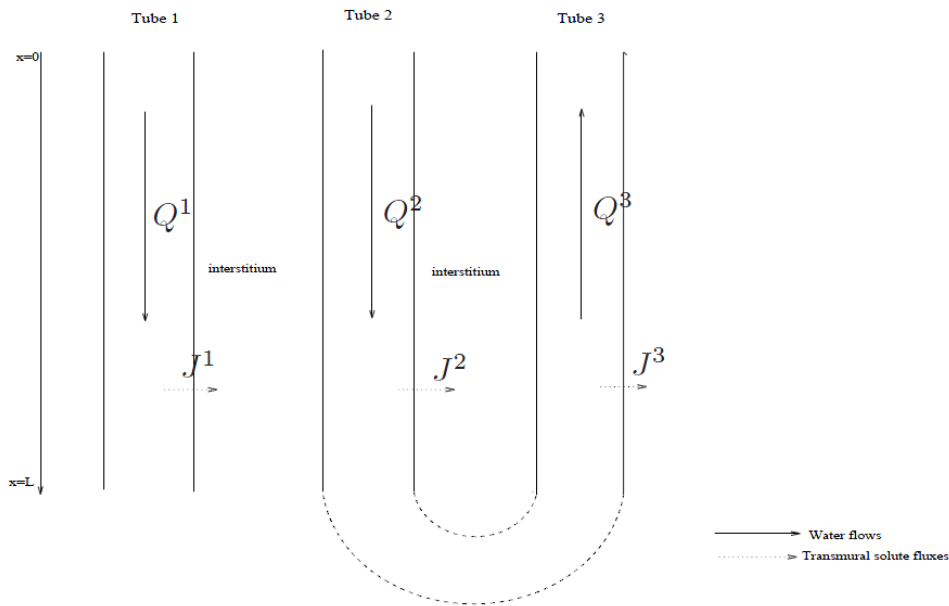


FIGURE 1. Simplified model of a nephron: Tube 1 represents a descending vasa recta or a collecting duct, tubes 2 and 3 represent descending and ascending limbs. Tubes are water-impermeable but can exchange solutes with the interstitium. These exchanges are quantified by the transmembrane fluxes J .

What makes this system specific and mathematically challenging is its unusual boundary conditions.

In the absence of transversal water movement, the main driving force for the transport of an uncharged solute is passive diffusion. In some kidney tubules there is also active transport, mediated by energy-consuming pumps that carry some solutes against their concentration gradient. We assume the presence of such a pump only in tube 3 (which is meant to represent the thick ascending limb), so that

$$\begin{cases} J^1(x) = 2\pi R^1(x)P^1(x)(C^{int}(x) - C^1(x)), \\ J^2(x) = 2\pi R^2(x)P^2(x)(C^{int}(x) - C^2(x)), \\ J^3(x) = 2\pi R^3(x)P^3(x)(C^{int}(x) - C^3(x)) - F(C^3(x), x), \end{cases} \quad (2)$$

where R^i and P^i respectively denote the radius and solute permeability of tube i , C^{int} is the interstitial concentration, and $F(C^3, x) > 0$ is a nonlinear term representing active transport, which is usually described using Michaelis-Menten kinetics

$$F(C^3, x) = V_m(x) \frac{C^3}{1 + C^3}. \tag{3}$$

Summarized in Table 1 are symbol definitions.

TABLE 1. Definition of frequently used symbols - Some parameter values depend on the depth x - The order of magnitude applies to rats

Parameter	Description	order of magnitude
$C^i(x)$	Solute concentration in tube i	5 mol.m^{-3}
$C^{int}(x)$	Solute concentration in the interstitium	5 mol.m^{-3}
C_0^1, C_0^2	Concentrations at the inlet of tubes 1 and 2	5 mol.m^{-3}
L	Length of the tubes	6.10^{-3} m
$Q^i(x)$	Water flow rate in tube i	$10^{-13} \text{ m}^3.\text{s}^{-1}$
$R^i(x)$	Radius of tube i	$5.10^{-5}.\text{m}$
$P^i(x)$	Solute permeability of the wall of tube i	10^{-5} m.s^{-1}
V_m	Rate of the active transport	$10^{-7} \text{ mol.m}^{-1}.\text{s}^{-1}$
$J^i(x)$	Transmural solute flux through the wall of tube i	

We then proceed to make the system non-dimensional. We define the dimensionless form of a generic variable A as:

$$\bar{A} = \frac{A}{A^0}$$

where A^0 is a constant on the same order of magnitude as A (see Table 1). We have

$$\bar{x} = \frac{x}{L^0}, \bar{C} = \frac{C}{C^0}, \bar{Q} = \frac{Q}{Q^0}, \bar{R} = \frac{R}{R^0}, \bar{P} = \frac{P}{P^0},$$

with L^0 to be defined.

Combining 1 with 2, we write, for $\bar{x} \in [0, \frac{L}{L^0}]$

$$\left\{ \begin{array}{l} Q^0 \bar{Q}^1 \frac{d(C^0 \bar{C}^1)}{L^0 d\bar{x}}(x) = 2\pi R^0 \bar{R}^1(x) P^0 \bar{P}^1(x) C^0 (\bar{C}^{int} - \bar{C}^1)(x), \\ Q^0 \bar{Q}^2 \frac{d(C^0 \bar{C}^2)}{L^0 d\bar{x}}(x) = 2\pi R^0 \bar{R}^2(x) P^0 \bar{P}^2(x) C^0 (\bar{C}^{int} - \bar{C}^2)(x), \\ Q^0 \bar{Q}^3 \frac{d(C^0 \bar{C}^3)}{L^0 d\bar{x}}(x) = 2\pi R^0 \bar{R}^3(x) P^0 \bar{P}^3(x) C^0 (\bar{C}^{int} - \bar{C}^3)(x) - F(\bar{C}^3(\bar{x}), \bar{x}), \\ \bar{C}^1(0) = \bar{C}_0^1, \quad \bar{C}^2(0) = \bar{C}_0^2, \quad \bar{C}^3(\frac{L}{L^0}) = \bar{C}^2(\frac{L}{L^0}), \end{array} \right.$$

To simplify the notation, we now drop the overbars (\bar{A}) and simply denote dimensionless variables as A . In addition, we assume that the radii, permeabilities, and flow rates are equal in all three tubes. Note that the flow is in the opposite direction in tube 3. We thus obtain

$$\left\{ \begin{array}{l} \frac{dC^1(x)}{dx} = P_s(C^{int}(x) - C^1(x)), \quad x \in [0, \frac{L}{L^0}], \\ \frac{dC^2(x)}{dx} = P_s(C^{int}(x) - C^1(x)), \quad x \in [0, \frac{L}{L^0}], \\ -\frac{dC^3(x)}{dx} = P_s(C^{int}(x) - C^3(x)) - F(C^3(x), x) \quad x \in [0, \frac{L}{L^0}], \\ C^1(0) = C_0^1, \quad C^2(0) = C_0^2, \quad C^3(\frac{L}{L^0}) = C^2(\frac{L}{L^0}), \end{array} \right. \quad (4)$$

where

$$P_s = \frac{2\pi L^0 R^0 P^0}{Q^0} \quad (5)$$

is a dimensionless effective solute permeability. We now choose L^0 so that $P_s = 1$. The nondimensional parameter $\frac{L}{L^0}$ (which is subsequently denoted L) is then about 200, and the nondimensional rate of active transport (which we still call V_m) is on the order of $\frac{L^0 V_m}{C^0 Q^0} = \frac{(3.10^{-5}).10^{-7}}{5.10^{-13}} \approx 5$.

Axial convection and diffusion are thought to be negligible in the renal interstitium. Since there is no accumulation of solute therein at steady state, we have

$$J^1(x) + J^2(x) + J^3(x) = 0. \quad (6)$$

This condition enables us to calculate the interstitial concentration explicitly

$$\forall x \in [0, L], \quad C^{int}(x) = \frac{1}{3} [C^1(x) + C^2(x) + C^3(x) + F(C^3(x), x)].$$

The goal of the study is to analyze and solve the following nonlinear boundary value problem set for $x \in [0, L]$

$$\left\{ \begin{array}{l} \frac{dC^1(x)}{dx} = \frac{1}{3} [C^1(x) + C^2(x) + C^3(x) + F(C^3(x), x)] - C^1(x), \\ \frac{dC^2(x)}{dx} = \frac{1}{3} [C^1(x) + C^2(x) + C^3(x) + F(C^3(x), x)] - C^2(x), \\ -\frac{dC^3(x)}{dx} = \frac{1}{3} [C^1(x) + C^2(x) + C^3(x) + F(C^3(x), x)] \\ \quad - C^3(x) - F(C^3(x), x), \\ C^1(0) = C_0^1, \quad C^2(0) = C_0^2, \quad C^3(L) = C^2(L). \end{array} \right. \quad (7)$$

This system represents the steady-state formulation of the standard dynamic problem [15] set for $t \geq 0$ and $x \in [0, L]$

$$\left\{ \begin{array}{l} \frac{\partial C^1}{\partial t}(x, t) + \frac{\partial C^1}{\partial x}(x, t) = \frac{1}{3} [-2C^1(x, t) + C^2(x, t) + C^3(x, t) + F(C^3(x, t), x)], \\ \frac{\partial C^2}{\partial t}(x, t) + \frac{\partial C^2}{\partial x}(x, t) = \frac{1}{3} [C^1(x, t) - 2C^2(x, t) + C^3(x, t) + F(C^3(x, t), x)], \\ \frac{\partial C^3}{\partial t}(x, t) - \frac{\partial C^3}{\partial x}(x, t) = \frac{1}{3} [C^1(x, t) + C^2(x, t) - 2C^3(x, t) - 2F(C^3(x, t), x)], \\ C^1(0, t) = C_0^1, \quad C^2(0, t) = C_0^2, \quad C^3(L, t) = C^2(L, t), \quad t > 0, \end{array} \right. \quad (8)$$

which we complete with nonnegative initial concentrations $C^1(x, 0)$, $C^2(x, 0)$, $C^3(x, 0)$. Implicit in this dynamic system is the assumption that the interstitium equilibrates immediately with its surroundings. In this study, we first prove that the solution to 8 converges, as t tends to ∞ , to the solution to 7 and that, under certain conditions, the convergence is exponential. We then use a finite volume scheme to solve 8 and thus approach the solution to 7. The numerical solution is subsequently employed to examine the effects of the countercurrent architecture on concentration gradients.

2. Main results. The main objective of this section is to study the long time convergence of the dynamic solution to the stationary solution. For this purpose, we describe the mathematical structure of the dynamic and stationary systems, state the natural properties of the dynamic solution, and infer a priori bounds for the latter solution which are time-independent. The proofs of the theorems outlined below are given in section 3. We follow the approach generally used to study relaxation systems, as in [16, 8], albeit with novel boundary conditions. We use the notation C for the vector function (C^1, C^2, C^3) .

2.1. Existence, uniqueness and a priori bounds. To ensure that the dynamic solution exists, we must make some assumptions regarding the nonlinear term representing active transport. We assume that the (smooth) function F satisfies for some (smooth) function $\mu(x) \geq 0$

$$F(C^3, x) \geq 0, \quad F(0, x) = 0, \quad 0 \leq F_C(C^3, x) \leq \mu(x) \leq \mu_M. \quad (9)$$

The Michaelis-Menten equation 3 which is generally used to represent active transport in the thick ascending limb can readily be shown to satisfy these 3 assumptions. The first one means that the pump can only transport solute in one direction, from the lumen of the thick ascending limb toward the interstitium. The second one describes the fact that there is no transport in the absence of solute. Lastly, the third assumption expresses the fact that the pump can be saturated because the number of carriers is limited.

Initial ($t = 0$) solute concentrations are positive. We further assume that, for $i = 1, 2$ or 3 ,

$$C^i(t = 0) \geq 0, \quad C^i(t = 0) \in L^1(0, L), \quad \frac{d}{dx} C^i(t = 0) \in L^1(0, L). \quad (10)$$

Another possible assumption is that the initial data are 'well-prepared', that is to say they match the boundary conditions

$$C^1(0, t = 0) = C_0^1, \quad C^2(0, t = 0) = C_0^2, \quad C^3(L, t = 0) = C^2(L, t = 0).$$

We do not use this assumption and thus handle possibly discontinuous solutions.

Theorem 2.1 (Existence and uniqueness of the dynamic problem solution). *With assumptions 9 and 10, there is a weak solution (defined in Appendix A) to the initial value problem 8, which lies in $BV([0, L] \times [0, T])$. For two initial data $C(x, 0)$ and $\tilde{C}(x, 0)$, the weak solutions satisfy the weak contraction property and the comparison principle*

$$\begin{aligned} \int_0^L [|C^1 - \tilde{C}^1| + |C^2 - \tilde{C}^2| + |C^3 - \tilde{C}^3|](x, t) dx \\ \leq \int_0^L [|C^1 - \tilde{C}^1| + |C^2 - \tilde{C}^2| + |C^3 - \tilde{C}^3|](x, 0) dx, \end{aligned} \quad (11)$$

$$\int_0^L [|C^1 - \tilde{C}^1|_+ + |C^2 - \tilde{C}^2|_+ + |C^3 - \tilde{C}^3|_+](x, t) dx \leq \int_0^L [|C^1 - \tilde{C}^1|_+ + |C^2 - \tilde{C}^2|_+ + |C^3 - \tilde{C}^3|_+](x, 0) dx. \tag{12}$$

For the latter inequality, we can assume that \tilde{C} is only a supersolution. The contraction property implies the uniqueness of the solution.

Theorem 2.2 (Stationary supersolution). *There is a family of supersolutions to 7, as large as needed, that are continuous functions U such that*

$$\begin{cases} \frac{dU^1(x)}{dx} + \frac{2}{3}U^1(x) - \frac{1}{3}[U^2(x) + U^3(x)] - \frac{1}{3}F(U^3(x), x) \geq 0, & (i) \\ \frac{dU^2(x)}{dx} + \frac{2}{3}U^2(x) - \frac{1}{3}[U^1(x) + U^3(x)] - \frac{1}{3}F(U^3(x), x) \geq 0, & (ii) \\ -\frac{dU^3(x)}{dx} + \frac{2}{3}U^3(x) + \frac{2}{3}F(U^3(x), x) - \frac{1}{3}[U^1(x) + U^2(x)] \geq 0, & (iii) \\ U^1(0) \geq C_0^1, \quad U^2(0) \geq C_0^2, \quad U^3(L) \geq U^2(L). \end{cases} \tag{13}$$

For initial data $C^i(x, 0) \leq U^i(x)$, then $C^i(x, t) \leq U^i(x)$ for all $t \geq 0$.

Theorem 2.3 (Uniform a priori estimates). *The weak solution to 8 satisfies*

$$\int_0^L [|\frac{\partial}{\partial t} C^1| + |\frac{\partial}{\partial t} C^2| + |\frac{\partial}{\partial t} C^3|](x, t) dx \leq A^0, \tag{14}$$

$$\sup_{0 \leq x \leq L} [C^1 + C^2 + C^3](x, t) \leq A^1, \tag{15}$$

$$\int_0^L [|\frac{\partial}{\partial x} C^1| + |\frac{\partial}{\partial x} C^2| + |\frac{\partial}{\partial x} C^3|](x, t) dx \leq A^2, \tag{16}$$

for some constants A^i depending only on the initial values $C^i(0, x)$ and their derivatives but not on t .

2.2. Long time behavior. Stationary problem. Our next results concern the problem we are interested in, that is the steady state and its stability. We begin with the

Theorem 2.4 (Existence of the stationary problem solution). *With assumptions 9, there is a unique solution to 7 which is C^1 and nonnegative.*

With the uniform bounds in Theorem 2.3, we can study the time convergence to this steady state.

Theorem 2.5 (Long time behavior and uniqueness of the stationary problem solution). *With assumptions 9, 10, the solution C to 8 converges to the unique solution \bar{C} to 7 in L^1 ,*

$$\|C(x, t) - \bar{C}(x)\|_{L^1} \underset{t \rightarrow \infty}{\searrow} 0.$$

Physiologically, this means that, whatever the initial solute concentrations, the system reaches the same steady state, that is, stationary concentration profiles are independent of initial values.

We can go further and study the rate of convergence toward the stationary solution. This requires some further notations and assumptions. For $\mu(x)$ defined in

9, we use the notations in Appendix C for the eigenelements $\phi = (\phi^1, \phi^2, \phi^3)$, $k(\mu)$ and $\Lambda(\mu)$. We assume

$$\sup_{x \in [0, L]} (2 - k(\mu))_+ [\mu(x) - F_C(C, x)] < \Lambda(\mu). \tag{17}$$

When $F(C, x) = \mu(x)C$, this condition is obviously satisfied and thus expresses a smallness condition on the second derivative in C .

When $F(C^3, x) = V_m(x) \frac{C^3}{1+C^3}$, the condition simplifies to

$$\sup_{x \in [0, L]} (2 - k(V_m))_+ V_m(x) < \Lambda(V_m), \tag{18}$$

which is a smallness condition on V_m since $\Lambda(0) > 0$.

With this assumption, we can state the

Theorem 2.6 (Exponential convergence). *With assumptions 9, 10 and 17, the solution to the problem 8 converges exponentially with t to the unique solution to 7 in the space*

$$L^1(\phi) = \left\{ f : [0, L] \rightarrow \mathbb{R}^3, \int_{[0, L]} (|f^1(x)|\phi^1(x) + |f^2(x)|\phi^2(x) + |f^3(x)|\phi^3(x)) dx < \infty \right\}.$$

that is to say:

$$\|C(x, t) - \bar{C}(x)\|_{L^1(\phi)} \leq e^{-\mu t} \|C(x, 0) - \bar{C}(x)\|_{L^1(\phi)}.$$

This theorem expresses a narrower result: if the maximal pump velocity V_m is small enough, the system reaches steady state at an exponential rate which depends on V_m . It is proved in Appendix C.

3. Proof of existence and a priori bounds. Because it is closely related to our numerical algorithm, and in order to introduce some basic concepts, we choose an approach based on the semi-discrete scheme.

3.1. Existence of a solution to the semi-discrete problem. Consider a discretisation parameter $\Delta x = L/N > 0$ with N an integer. The semi-discrete scheme associated with 8 is defined, for $k \in [1, N]$, as

$$\begin{cases} \frac{dC_k^1}{dt}(t) + \frac{C_k^1(t) - C_{k-1}^1(t)}{\Delta x} = \frac{1}{3} [C_k^1(t) + C_k^2(t) + C_k^3(t) + F(C_k^3(t))] - C_k^1(t), \\ \frac{dC_k^2}{dt}(t) + \frac{C_k^2(t) - C_{k-1}^2(t)}{\Delta x} = \frac{1}{3} [C_k^1(t) + C_k^2(t) + C_k^3(t) + F(C_k^3(t))] - C_k^2(t), \\ \frac{dC_k^3}{dt}(t) - \frac{C_{k+1}^3(t) - C_k^3(t)}{\Delta x} = \frac{1}{3} [C_k^1(t) + C_k^2(t) + C_k^2(t) + F(C_k^3(t))] - C_k^3(t) - F(C_k^3(t)), \end{cases} \tag{19}$$

with the boundary conditions $C_0^1 > 0$ and $C_0^2 > 0$ given in 8 and $C_{N+1}^3 = C_N^2$. We also choose the initial data

$$C_k^i(0) = \frac{1}{\Delta x} \int_{(k-1)\Delta x}^{k\Delta x} C^i(x, 0) dx, \quad i = 1, 2, 3, \quad k = 1, \dots, N. \tag{20}$$

Because 19 is a system of differential equations, it has a unique smooth solution and it is nonnegative. Indeed, if there exists (i, k, t) (for instance $i = 1$ without loss of generality) where

$$t = \inf\{s \text{ such that } \exists(k, i) \text{ satisfying } C_k^i(s) = 0\},$$

then,

$$\frac{dC_k^1}{dt}(t) = \frac{C_{k-1}^1(t)}{\Delta x} + \frac{1}{3}\left(C_k^2(t) + C_k^3(t) + F(C_k^3(t))\right) \geq 0.$$

So, $C_k^1(t)$ cannot become negative.

In order to link the continuous model to this discrete equation, we reconstruct three piecewise constant functions $C_{\Delta x}^i(x, t)$, from the discrete values, as

$$C_{\Delta x}^i(x, t) = C_k^i(t), \quad \text{for } x \in ((k - 1)\Delta x, k\Delta x), \quad i = 1, 2, 3. \quad (21)$$

To simplify the notation, we sometimes merely write C instead of $C_{\Delta x}$. We next prove that $C_{\Delta x}$ converges to the continuous solution.

Our proof is divided in several steps. We first recall some preliminary estimates on $C_k^i(0)$. Secondly we derive several uniform (in Δx) a priori bounds on the semi-discrete solutions. Thirdly, we use these estimates to prove that the solution converges when Δx goes to 0 to a weak solution to 8. Then, still using a priori bounds, we find some additional properties of the solution. These are enough to pass to the limit and recover a weak solution to 8.

First step. Preliminary controls. Given our assumptions 10, we derive using a classic approach (see [2, 7, 14]) the following initial bounds at the discrete level

$$\|C_{\Delta x}(t = 0)\|_{L^1} \leq K^0 := \sum_{i=1}^3 \|C^i(t = 0)\|_{L^1}, \quad (22)$$

$$\sum_{i=1}^3 \sum_{k=1}^N \|C_k^i(t = 0) - C_{k-1}^i(t = 0)\|_{L^1} \leq K^1 := \sum_{i=1}^3 \left\| \frac{d}{dx} C^i(t = 0) \right\|_{M^1}, \quad (23)$$

$$\left\| \frac{d}{dt} C_{\Delta x}(t = 0) \right\|_{L^1} \leq K^2, \quad (24)$$

for a constant K^2 , obtained from the equation and using 22-23, which only depends on the initial data but not on Δx . Here, M^1 is the Banach space of bounded measures. Indeed, from 19, we deduce that for $k \in [1, N]$ we have

$$\begin{aligned} \left\| \frac{dC}{dt}(0) \right\|_{L^1} &\leq \sum_{k=1}^N |C_k^1(0) - C_{k-1}^1(0)| + \sum_{k=1}^N |C_k^2(0) - C_{k-1}^2(0)| \\ &\quad + \sum_{k=1}^N |C_k^3(0) - C_{k+1}^3(0)| + \frac{4}{3}(\mu_M + 1)\|C(0)\|_{L^1} \end{aligned} \quad (25)$$

because μ is bounded on $[0, L]$ by μ_M .

On the other hand 23 holds true. The notation $\|\cdot\|_{M^1}$ includes a Dirac mass at $x = 0$ for $i = 1, 2$, when the initial data do not match the boundary condition. Indeed, applying 10 to C^1 , and based upon 20, we can write

$$\begin{aligned}
 \sum_{k=1}^N |C_k^1(0) - C_{k-1}^1(0)| &= \frac{1}{\Delta x} \sum_{k=2}^N \left| \int_{(k-1)\Delta x}^{k\Delta x} C^1(x, 0) dx \right. \\
 &\quad \left. - \int_{(k-2)\Delta x}^{(k-1)\Delta x} C^1(x, 0) dx + \int_0^{\Delta x} (C^1(x, 0) - C_0^1) dx \right| \\
 \sum_{k=1}^N |C_k^1(0) - C_{k-1}^1(0)| &= \frac{1}{\Delta x} \sum_{k=2}^N \left[\left| \int_{(k-1)\Delta x}^{k\Delta x} [C^1(x, 0) dx - C^1(x - \Delta x, 0)] dx \right. \right. \\
 &\quad \left. \left. + \int_0^{\Delta x} (C^1(x, 0) - C_0^1) dx \right| \right] \\
 &= \frac{1}{\Delta x} \sum_{k=2}^N \left[\left| \int_{(k-1)\Delta x}^{k\Delta x} \int_{x-\Delta x}^x \frac{d}{dx} C^1(z, 0) dz dx \right| + \left| \int_0^{\Delta x} \int_0^x \frac{d}{dx} C^1(z, 0) dz dx \right| \right] \\
 &\leq \frac{1}{\Delta x} \sum_{k=2}^N \left[\int_{(k-1)\Delta x}^{k\Delta x} \int_0^{\Delta x} \left| \frac{d}{dx} C^1(x + u - \Delta x, 0) \right| du dx \right. \\
 &\quad \left. + \int_0^{\Delta x} \int_0^x \left| \frac{d}{dx} C^1(z, 0) \right| dz dx \right] \\
 &\leq \frac{1}{\Delta x} \left[\int_0^{\Delta x} \int_{\Delta x}^L \left| \frac{d}{dx} C^1(x + u - \Delta x, 0) \right| dx du + \int_0^{\Delta x} \int_0^x \left| \frac{d}{dx} C^1(z, 0) \right| dz dx \right] \\
 &\leq \frac{1}{\Delta x} \left[\int_0^{\Delta x} \int_x^{L+x-\Delta x} \left| \frac{d}{dx} C^1(z, 0) \right| dz dx + \int_0^{\Delta x} \int_0^x \left| \frac{d}{dx} C^1(z, 0) \right| dz dx \right] \\
 &\leq \frac{1}{\Delta x} \int_0^{\Delta x} \int_0^{L+x-\Delta x} \left| \frac{d}{dx} C^1(z, 0) \right| dz dx \\
 &\leq \left\| \frac{d}{dx} C^1(t = 0) \right\|_{L^1}.
 \end{aligned}$$

□

Second step. Control in time. We first prove a uniform control on time derivatives

$$\left\| \frac{dC_{\Delta x}}{dt}(t) \right\|_{L^1} \leq \left\| \frac{dC_{\Delta x}}{dt}(0) \right\|_{L^1} \leq K^2, \quad \forall t > 0. \tag{26}$$

To prove this, we differentiate 19 with respect to t , we multiply each line i by $\text{sign}(\frac{d}{dt} C_k^i)$ and find

$$\begin{cases}
 \frac{d}{dt} \left| \frac{dC_k^1}{dt} \right| + \frac{1}{\Delta x} \left[\left| \frac{dC_k^1}{dt} \right| - \left| \frac{dC_{k-1}^1}{dt} \right| \right] \\
 \leq \frac{1}{3} \left(-2 \left| \frac{dC_k^1}{dt} \right| + \left| \frac{dC_k^2}{dt} \right| + \left| \frac{dC_k^3}{dt} \right| + \left| \frac{dC_k^3}{dt} \frac{\partial F}{\partial C} \right| \right), \\
 \frac{d}{dt} \left| \frac{dC_k^2}{dt} \right| + \frac{1}{\Delta x} \left[\left| \frac{dC_k^2}{dt} \right| - \left| \frac{dC_{k-1}^2}{dt} \right| \right] \leq \frac{1}{3} \left(\left| \frac{dC_k^1}{dt} \right| - 2 \left| \frac{dC_k^2}{dt} \right| + \left| \frac{dC_k^3}{dt} \right| + \left| \frac{dC_k^3}{dt} \frac{\partial F}{\partial C} \right| \right), \\
 \frac{d}{dt} \left| \frac{dC_k^3}{dt} \right| + \frac{1}{\Delta x} \left[\left| \frac{dC_k^3}{dt} \right| - \left| \frac{dC_{k+1}^3}{dt} \right| \right] \leq \frac{1}{3} \left(\left| \frac{dC_k^1}{dt} \right| + \left| \frac{dC_k^2}{dt} \right| - 2 \left| \frac{dC_k^3}{dt} \right| - 2 \left| \frac{dC_k^3}{dt} \frac{\partial F}{\partial C} \right| \right).
 \end{cases}$$

We sum on the lines and on the indices k to obtain

$$\begin{aligned} \frac{d}{dt} \sum_{k=1}^N \sum_{i=1}^3 \Delta x \left| \frac{d}{dt} C_k^i(t) \right| &\leq - \left| \frac{d}{dt} C_N^1(t) \right| + \left| \frac{d}{dt} C_0^1 \right| - \left| \frac{d}{dt} C_N^2(t) \right| + \left| \frac{d}{dt} C_0^2 \right| \\ &\quad + \left| \frac{d}{dt} C_{N+1}^3(t) \right| - \left| \frac{d}{dt} C_1^3 \right|. \end{aligned}$$

Knowing that C_0^1 and C_0^2 are independent of t , we have $\frac{d}{dt} C_0^1 = 0$, $\frac{d}{dt} C_0^2 = 0$. In addition, since $C_{N+1}^3(t) = C_N^2(t)$, we have $\frac{d}{dt} C_{N+1}^3(t) = \frac{d}{dt} C_N^2(t)$. Altogether, we arrive at

$$\frac{d}{dt} \sum_{k=1}^N \Delta x \left[\left| \frac{d}{dt} C_k^1(t) \right| + \left| \frac{d}{dt} C_k^2(t) \right| + \left| \frac{d}{dt} C_k^3(t) \right| \right] \leq 0. \quad (27)$$

That proves our first estimate 26.

Third step. Bounds on $C_{\Delta x}$. Our purpose here is to prove that we also have for all $t \geq 0$

$$\|C_{\Delta x}(t)\|_{L^1} \leq K^0 + K^3 t, \quad \text{with } K^3 = C_0^1 + C_0^2. \quad (28)$$

To do so, using 19, we sum on the lines and on the indices and find

$$\frac{d}{dt} \sum_{k=1}^N \Delta x \left[C_k^1(t) + C_k^2(t) + C_k^3(t) \right] \leq C_0^2 + C_0^1 \quad (29)$$

and the result follows.

Fourth step. Uniform bounded variations on $C_{\Delta x}$. We want to prove the uniform BV control

$$\sum_{k=1}^N |C_k - C_{k-1}|(t) \leq K^4(1+t) \quad \forall t > 0. \quad (30)$$

Note that an uniform bound follows directly from this BV control. For all $t \geq 0$,

$$C_k^i \leq C_0^i + K^4(1+t), \quad i = 1, 2, \quad C_k^3 \leq C_0^2 + 2K^4(1+t). \quad (31)$$

We prove it for C^1 only. We deduce from 19 that

$$\begin{aligned} \sum_{k=1}^N |C_k^1 - C_{k-1}^1|(t) &\leq \sum_{k=1}^N \Delta x \left| \frac{d}{dt} C_k^1(t) \right| + \sum_{k=1}^N \frac{\Delta x}{3} \left[2|C_k^1| + |C_k^2| + (1 + \mu_M)|C_k^3| \right](t) \\ &\leq K^4(1+t) \end{aligned}$$

using the estimates 28 and 26.

Fifth step. Convergence of the semi-discrete solution. Because we have proved that $C_{\Delta x}$ is uniformly bounded in $BV([0, T] \times [0, L])$, according to the Rellich-Kondrachov compactness theorem (see [4, 3]), there is a subsequence which converges in $L^1((0, T) \times (0, L))$ to a function $C(x, t) \in L^1((0, T) \times (0, L))$. Then, after further extracting a subsequence we obtain

$$C_{\Delta x}(x, t) \xrightarrow{\Delta x \rightarrow 0} C(x, t), \quad a.e.$$

Consequently we also have, because F is continuous in C^3 ,

$$F(C_{\Delta x}^3(x, t), x) \xrightarrow{\Delta x \rightarrow 0} F(C^3(x, t), x).$$

To check that this limit is a weak solution to 8, we introduce the set V of test-functions

$$V = \left\{ \Phi \in \left(C^1(\mathbb{R}^+ \times [0, L]) \right)^3, \quad \Phi^1(L, t) = \Phi^3(0, t) = 0, \quad \Phi^3(L, t) = \Phi^2(L, t) \right\}. \tag{32}$$

It is easy to pass to the limit in the zero order terms because, using the dominated convergence theorem, we have, for all $\Phi \in V$

$$\begin{aligned} \int_0^T \int_0^L C_{\Delta x}^j(x, t) \Phi^j(x, t) dx dt &\xrightarrow{\Delta x \rightarrow 0} \int_0^T \int_0^L C^j(x, t) \Phi^j(x, t) dx dt, \\ \int_0^T \int_0^L F(C_{\Delta x}^3(x, t), x) \Phi^3(x, t) dx dt &\xrightarrow{\Delta x \rightarrow 0} \int_0^T \int_0^L F(C^3(x, t), x) \Phi^3(x, t) dx dt. \end{aligned}$$

To recover the terms with x -derivatives is more difficult. After a change of variable, we write

$$\begin{aligned} &\int_0^T \int_{\Delta x}^L \frac{C_{\Delta x}^1(x, t) - C_{\Delta x}^1(x - \Delta x, t)}{\Delta x} \Phi^1(x, t) dx dt \\ &= \int_0^T \int_{\Delta x}^L \frac{C_{\Delta x}^1(x, t)}{\Delta x} \Phi^1(x, t) dx dt - \int_0^T \int_0^{L-\Delta x} \frac{C_{\Delta x}^1(x, t)}{\Delta x} \Phi^1(x + \Delta x, t) dx dt \\ &= - \int_0^T \int_0^{\Delta x} \frac{C_{\Delta x}^1(x, t)}{\Delta x} \Phi^1(t, x) dx dt \\ &\quad + \int_0^T \int_0^{L-\Delta x} C_{\Delta x}^1(x, t) \frac{\Phi^1(x, t) - \Phi^1(x + \Delta x, t)}{\Delta x} dx dt \\ &\quad + \int_0^T \int_{L-\Delta x}^L \frac{C_{\Delta x}^1(x, t)}{\Delta x} \Phi^1(x, t) dx dt. \end{aligned}$$

Using again the dominated convergence theorem, we have

$$\begin{aligned} &\int_0^T \int_{\Delta x}^{L-\Delta x} C_{\Delta x}^1(x, t) \frac{\Phi^1(x, t) - \Phi^1(x + \Delta x, t)}{\Delta x} dx dt \\ &\xrightarrow{\Delta x \rightarrow 0} - \int_0^T \int_0^L C^1(x, t) \frac{\partial \Phi^1(x, t)}{\partial x} dx dt, \\ &- \int_0^T \int_0^{\Delta x} \frac{C_{\Delta x}^1(x, t)}{\Delta x} \Phi^1(x + \Delta x, t) dx dt \xrightarrow{\Delta x \rightarrow 0} - \int_0^T \Phi^1(0, t) C^1(0, t), \\ &\int_0^T \int_{L-\Delta x}^L \frac{C_{\Delta x}^1(x, t)}{\Delta x} \Phi^1(x, t) dx dt \xrightarrow{\Delta x \rightarrow 0} \int_0^T \Phi^1(L, t) C^1(L, t) = 0. \end{aligned}$$

Integrating by part, we obtain

$$\begin{aligned} \int_0^T \int_0^L \frac{\partial C_{\Delta x}^1(x, t)}{\partial t} \Phi^1(x, t) dx dt &= \xrightarrow{\Delta x \rightarrow 0} - \int_0^T \int_0^L C^1(x, t) \frac{\partial \Phi^1(x, t)}{\partial t} dx dt \\ &\quad + \int_0^L \Phi^1(x, T) C^1(x, T) dx - \int_0^L \Phi^1(x, 0) C^1(x, 0) dx. \end{aligned}$$

We are now ready to pass to the limit in the equations. We treat each component of the system independently. The equation satisfied by $C_{\Delta x}^1$ is

$$\left\{ \begin{array}{l} \frac{\partial C_{\Delta x}^1}{\partial t}(x, t) + \frac{C_{\Delta x}^1(x, t) - C_{\Delta x}^1(t, x - \Delta x)}{\Delta x} = -\frac{2}{3}C_{\Delta x}^1(x, t) \\ \quad + \frac{1}{3} [C_{\Delta x}^2(x, t) + C_{\Delta x}^3(x, t) + F(C_{\Delta x}^3(x, t), x)], \quad x \in]\Delta x, L], \\ \frac{\partial C_{\Delta x}^1}{\partial t}(x, t) + \frac{C_{\Delta x}^1(x, t) - C_0^1}{\Delta x} = -\frac{2}{3}C_{\Delta x}^1(x, t) \\ \quad + \frac{1}{3} [C_{\Delta x}^2(x, t) + C_{\Delta x}^3(x, t) + F(C_{\Delta x}^3(x, t), x)], \quad x \in]0, \Delta x], \\ C_{\Delta x}^1(0, t) = C_0^1, \quad x = 0. \end{array} \right. \tag{33}$$

The equations for C^2 and C^3 are treated similarly, because the boundary conditions are related and cancel out when the equations are added. Thus, we prove that C satisfies the following weak formulation.

We subsequently prove that the first line of 33 converges to a weak equation, and deduce the weak equation satisfied by C .

3.2. Properties of limit. In the limit process, we keep the a priori bounds that we record here from 26, 28, 30

$$\int_0^L [C^1 + C^2 + C^3](x, t)dx \leq K^0 + K^3t, \quad \forall t \geq 0, \tag{34}$$

$$\int_0^L [|\frac{\partial}{\partial t}C^1| + |\frac{\partial}{\partial t}C^2| + |\frac{\partial}{\partial t}C^3|](x, t)dx \leq K^2, \quad \forall t \geq 0, \tag{35}$$

$$\|\frac{\partial C}{\partial x}(t)\|_{L^1[0, L]} \leq K^4(1 + t) \quad \forall t \geq 0. \tag{36}$$

Moreover, we can prove that C is uniformly continuous in time. Indeed, $\forall t > 0, h > 0$,

$$\begin{aligned} \|C(x, t + h) - C(x, t)\|_{L^1[0, L]} &\leq \int_0^L \left| \int_0^h \frac{\partial}{\partial t} C(x, t + s) ds \right| dx \\ &\leq \int_0^h \left\| \frac{d}{dt} C(x, t + s) \right\|_{L^1[0, L]} ds \leq K^0 h. \end{aligned}$$

□

This proves that for all $T > 0$ the regularity holds also

$$C^i \in C([0, T]; L^1[0, L]) \cap BV([0, T] \times [0, L]).$$

The drawback of estimates 34 and 36 is that they are time-dependent. This is improved in section 3.4.

3.3. The contraction property and the comparison principle. We continue this section with the contraction property 11. We use the notations

$$d^i(x, t) := |C^i(x, t) - \tilde{C}^i(x, t)|, \quad i = 1, 2, 3.$$

$$G(x, t) := |F(C^3(x, t), x) - F(\tilde{C}^3(x, t), x)| \leq \mu(x) d^3(x, t).$$

We subtract the lines i in 8 for C and \tilde{C} . We multiply them by $\text{sign}(C^i(x, t) - \tilde{C}^i(x, t))$, (see [1, 17] and the references therein). We obtain the inequalities

$$\begin{cases} \frac{\partial d^1}{\partial t} + \frac{\partial d^1}{\partial x} \leq -\frac{2}{3}d^1 + \frac{1}{3}(d^2 + d^3 + G), \\ \frac{\partial d^2}{\partial t} + \frac{\partial d^2}{\partial x} \leq -\frac{2}{3}d^2 + \frac{1}{3}(d^1 + d^3 + G), \\ \frac{\partial d^3}{\partial t} - \frac{\partial d^3}{\partial x} \leq -\frac{2}{3}(d^3 + G) + \frac{1}{3}(d^2 + d^1). \end{cases} \tag{37}$$

The third line uses the fact that, because we assume F is nondecreasing in C (assumption 9)

$$\begin{aligned} & \text{sign}(C^3(x, t) - \tilde{C}^3(x)) \left[F(C^3(x, t), x) - F(\tilde{C}^3(x), x) \right] \\ &= \left| F(C^3(x, t), x) - F(\tilde{C}^3(x), x) \right|. \end{aligned}$$

From these inequalities we conclude that

$$\frac{d}{dt} \int_0^L [d^1 + d^2 + d^3] dx \leq -d^1(L, t) - d^3(0, t) \leq 0, \tag{38}$$

which implies

$$\int_0^L [d^1(x, t) + d^2(x, t) + d^3(x, t)] dx \leq \int_0^L [d^1(x, 0) + d^2(x, 0) + d^3(x, 0)] dx. \tag{39}$$

This is the contraction property 11.

The variant 12 can be proved following the same calculation, multiplying line i by $\text{sign}_+ (\tilde{C}^i(x, t) - C^i(x, t))$, defined by $\text{sign}_+(f) = \text{sign}(\max(f, 0))$. Because sign_+ is increasing, it is enough to work with a supersolution $\tilde{C}^i(x, t)$.

3.4. Proof of Theorem 2.3 and supersolution. We first build the family of stationary supersolutions, then we derive the uniform bounds on $C(x, t)$.

First step. A family of supersolution to 7. Our goal is to build nonnegative functions U^1, U^2, U^3 such that $U^3(x) = U^1(x) + U^2(x)$ and U^1, U^2 satisfy

$$\begin{cases} \frac{dU^1(x)}{dx} + \frac{1}{3}U^1(x) - \frac{2}{3}U^2(x) - \frac{1}{3}F(U^1(x) + U^2(x), x) = 0, \\ \frac{dU^2(x)}{dx} + \frac{1}{3}U^2(x) - \frac{2}{3}U^1(x) - \frac{1}{3}F(U^1(x) + U^2(x), x) = 0, \\ U^1(0) \geq C_0^1, \quad U^2(0) \geq C_0^2. \end{cases} \tag{40}$$

which is clearly sufficient to have a supersolution to 7.

For U^3 , summing the equations on U^1 and U^2 , we obtain

$$\frac{d}{dx} [U^1(x) + U^2(x)] - \frac{1}{3} [U^1(x) + U^2(x)] - \frac{2}{3} F(U^1(x) + U^2(x), x) = 0,$$

so that we also have

$$-\frac{dU^3(x)}{dx} + \frac{2}{3}U^3(x) + \frac{2}{3}F(U^3(x), x) - \frac{1}{3} [U^1(x) + U^2(x)] = 0,$$

which implies that the correct equation holds. The boundary condition is also satisfied as a supersolution because $U^3(L) = U^2(L) + U^1(L) \geq U^2(L)$.

To build a supersolution to 40, we choose $U^1 = U^2 = \frac{1}{2}H$, where H satisfies

$$\frac{dH(x)}{dx} - \frac{1}{3}H(x) - \frac{2}{3}F(H(x), x) = 0, \quad H(0) = 2 \max(C_0^1, C_0^2). \quad (41)$$

We conclude the proof because 41 is solved by the Cauchy-Lipschitz theorem. Note that the boundary condition $H(0) = H^0$ in place of $2 \max(C_0^1, C_0^2)$ allows us to find U^1 and U^2 (and thus U^3) as large as we want. \square

Second step. Uniform L^∞ bounds on $C^i(x, 0)$. From the comparison principle 12, we conclude that $C(x, t) \leq U^i(x)$ choosing, as indicated above, $U^i(x) \geq C^i(x, 0)$. This proves 15.

From this uniform a priori bound, we also deduce 16 which improves 36. \square

3.5. Proof of Theorem 2.4 (existence of a solution to the stationary problem). We prove the existence of a solution to 7. To do so, we use an auxiliary boundary value problem which is studied in Appendix B,

$$\begin{cases} \frac{dC^1(x)}{dx} + \frac{2}{3}C^1(x) = \frac{1}{3} [C^2(x) + C^3(x) + F(C^3(x), x)], \\ \frac{dC^2(x)}{dx} + \frac{2}{3}C^2(x) = \frac{1}{3} [C^1(x) + C^3(x) + F(C^3(x), x)], \\ -\frac{dC^3(x)}{dx} + \frac{2}{3} [C^3(x) + F(C^3(x), x)] = \frac{1}{3} [C^1(x) + C^2(x)], \\ C^1(0) = C_0^1 > 0, \quad C^2(0) = C_0^2 > 0, \quad C^3(L) = C_L^3 \geq 0. \end{cases} \quad (42)$$

For theorem 2.4, it is enough to prove that there is a positive value C_L^3 such that the solution to 42 satisfies $C^3(L) = C^2(L)$. To do so, we define the continuous mapping

$$g : C_L^3 \mapsto C^2(L) - C^3(L)$$

We claim that $g(0) > 0$ and that $g(\infty) < 0$, which implies that g vanishes on \mathbb{R}^+ and concludes the proof.

- $g(0) > 0$. By the maximum principle, the $C^i(\cdot)$ are nonnegative and since C_0^2 is positive, so is $C^2(L)$.
- $g(\infty) < 0$. We want to prove that for C_L^3 large enough $C^2(L) < C^3(L)$. It is enough to prove that

$$C^1(L) + C^2(L) < C^3(L). \quad (43)$$

Because solutions to 42 satisfy

$$\frac{d}{dx} [C^1 + C^2 - C^3] = 0,$$

proving 43 is equivalent to proving that

$$C_0^1 + C_0^2 < C^3(0). \quad (44)$$

But this is obvious because, since the C^i s are nonnegative, we have $C^3(x) \geq C^3(L) \exp(-2(1 + \mu_M)(L - x)/3)$. This concludes the existence proof.

Uniqueness follows again from the contraction property 38 which for time independent solutions proves that the three components coincide at $x = 0$. \square

3.6. Proof of Theorem 2.5 (large time limit). Our proof is organized as follows. We consider the case where the initial data is a sub- or a supersolution to the steady state equation 7; we prove that the solutions are monotonic in time and, because they are bounded as stated in theorem 2.3, they converge to the steady state. This is enough because for any initial data, we can always use theorem 2.2 and find a supersolution U_0 such that

$$0 \leq C^i(x, 0) \leq U_0^i(x) \quad \forall i, \forall x \in [0, L].$$

Calling V and U the solutions to 8 with respective initial conditions taken to be $V_0 = 0$ (a subsolution!) and U_0 , we obtain according to the comparison principle

$$V^i(x, t) \leq C^i(x, t) \leq U^i(x, t) \quad \forall i, \forall x \in [0, L], \forall t > 0.$$

As U and V converge toward the steady state, so does C .

With this argument we are reduced to proving theorem 2.5 with initial data $C(., t = 0)$ that are supersolution to 7; indeed the same argument holds for subsolutions where the only modification consists in replacing the $\left(\frac{\partial C}{\partial t}\right)_+$ with $\left(\frac{\partial C}{\partial t}\right)_-$.

First step. In the same way that we established the first inequality of theorem 2.3, we can differentiate 8 with respect to t , multiply each line i by $\text{sign}_+\left(\frac{\partial C^i}{\partial t}\right)$ (defined in section 3.3), and sum on the lines. We obtain the variant of 14

$$\frac{d}{dt} \int_0^L \left[\left(\frac{\partial C^1}{\partial t}\right)_+ + \left(\frac{\partial C^2}{\partial t}\right)_+ + \left(\frac{\partial C^3}{\partial t}\right)_+ \right] (x, t) dt \leq 0. \quad (45)$$

Second step. As $C(., t = 0)$ is a supersolution, we have $\left(\frac{\partial C^i}{\partial t}(x, 0)\right)_+ = 0$ for all i , $x \in [0, L]$. Using 45, we conclude that

$$\left(\frac{\partial C^i}{\partial t}(x, t)\right)_+ = 0 \quad \forall i, \forall x \in [0, L], \forall t > 0,$$

which means that $C(., t)$ is a supersolution of 7 for all $t > 0$ and that each component is monotonically decreasing.

Therefore we can pass to the limit pointwise as $t \rightarrow \infty$ and $C^i(x, t)$ converges to a function $\bar{C}^i(x)$. Because time derivatives converge to 0 in the distributional sense, $\bar{C}(x)$ is the stationary solution and thus coincides with that built in theorem 2.4.

This establishes theorem 2.5 for initial data which are supersolutions and thus concludes the proof. \square

4. Numerical method. Since, at least for small nonlinearities, the solution to the dynamic problem converges exponentially toward the steady state solution, we propose to approach numerically the solution to 7 by computing the solution to 8 for large times. For simplicity, we only treat the Michaelis-Menten form of the active transport term 3. Also, as is usually done with in transport equations, we use a finite volume method (see [2, 14, 7]).

4.1. The finite volume scheme. We use a time step Δt and a mesh of size $\Delta x = L/N$ with N the number of cells $Q_k = (x_{k-1/2}, x_{k+1/2})$ (that means $x_{1/2} = 0$ and $x_{N+1/2} = L$). The discrete times are denoted by $t^n = n\Delta t$. To guarantee that the discrete solution remains nonnegative as shown later, we use the CFL condition

$$\Delta t \leq \frac{3\Delta x}{3 + 2\Delta x + 2\Delta x V_m}. \quad (46)$$

The principle of finite volumes is to enforce numerical conservation of quantities that are physically conserved and thus to approximate quantities by their average. For instance the discrete initial states are, as before

$$C_k^{i,0} = \frac{1}{\Delta x} \int_{Q_k} C^i(x,0)dx, \quad i = 1, 2, 3, \quad k = 1, \dots, N. \tag{47}$$

We call $C_k^{i,n}$ the discrete solution at time t^n in tube i that approximates equation 8, for $k \in [0, N]$. We use the scheme

$$\begin{cases} C_k^{1,n+1} = C_k^{1,n} - \frac{\Delta t}{\Delta x}(C_k^{1,n} - C_{k-1}^{1,n}) + \Delta t J_k^{1,n}, \\ C_k^{2,n+1} = C_k^{2,n} - \frac{\Delta t}{\Delta x}(C_k^{2,n} - C_{k-1}^{2,n}) + \Delta t J_k^{2,n}, \\ C_k^{3,n+1} = C_k^{3,n} + \frac{\Delta t}{\Delta x}(C_{k+1}^{3,n} - C_k^{3,n}) + \Delta t J_k^{3,n}, \end{cases} \tag{48}$$

with the notations

$$\begin{cases} C_k^{int,n} = \frac{1}{3} \left[C_k^{1,n} + C_k^{2,n} + C_k^{3,n} + V_m \frac{C_k^{3,n}}{1 + C_k^{3,n}} \right], \\ J_k^{1,n} = C_k^{int,n} - C_k^{1,n}, \quad J_k^{2,n} = C_k^{int,n} - C_k^{2,n}, \\ J_k^{3,n} = C_k^{int,n} - C_k^{3,n} - V_m \frac{C_k^{3,n}}{1 + C_k^{3,n}}. \end{cases} \tag{49}$$

For boundary conditions, at each time we choose: $C_0^{1,n} = C_0^1$, $C_0^{2,n} = C_0^2$, $C_{N+1}^{3,n} = C_N^{2,n}$.

Because this is an explicit scheme, departing from 47, we obtain directly the solution $C_k^{1,n+1}$ at time t^{n+1} from that at time t^n .

Derivation of the CFL condition. In order to guarantee that the discrete solution remains nonnegative, under the assumptions that the boundary conditions and the initial conditions are nonnegative, we assume that

$$\forall i \in [1, 2, 3], \forall k \in [1, N], C_k^{i,n} \geq 0.$$

We seek to have the same property for the following step of time:

$$\forall i \in [1, 2, 3], \forall k \in [1, N], C_k^{i,n+1} \geq 0.$$

We begin with $C_k^{1,n+1}$ and we write 48 as

$$C_k^{1,n+1} = \left[1 - \frac{2}{3}\Delta t - \frac{\Delta t}{\Delta x} \right] C_k^{1,n} + \frac{\Delta t}{\Delta x} C_{k-1}^{1,n} + \frac{\Delta t}{3} C_k^{2,n} + \frac{\Delta t}{3} C_k^{3,n} + \frac{\Delta t}{3} V_m \frac{C_k^{3,n}}{1 + C_k^{3,n}}.$$

To insure that $C_k^{1,n+1}$ is a positive combination of positive terms, we have to impose $1 - \frac{2}{3}\Delta t - \frac{\Delta t}{\Delta x} \geq 0$, that is to say

$$\Delta t \leq \frac{3\Delta x}{2\Delta x + 3}. \tag{50}$$

The same argument holds for C^2 . For C^3 , we write

$$C_k^{3,n+1} = \left[1 - \frac{2}{3}\Delta t - \frac{\Delta t}{\Delta x} - \frac{2}{3} V_m \frac{\Delta t}{1 + C_k^{3,n}} \right] C_k^{3,n} + \frac{\Delta t}{\Delta x} C_{k+1}^{3,n} + \frac{\Delta t}{3} C_k^{2,n} + \frac{\Delta t}{3} C_k^{1,n}.$$

Here we have to impose that

$1 - \frac{2}{3}\Delta t - \frac{\Delta t}{\Delta x} - \frac{2}{3}V_m \frac{\Delta t}{1+C_k^{3,n}} \geq 0$, that is to say

$$\Delta t \leq \frac{3\Delta x}{3 + 2\Delta x + 2\Delta x V_m} \leq \frac{3\Delta x}{2\Delta x + 3}. \tag{51}$$

Finally, to satisfy both 50 and 51, it is sufficient to impose 46. \square

The arguments developed for the continuous model can be used at the discrete level to prove that the numerical solutions remain bounded, as we now describe.

Stability of the scheme. We want to guarantee, under the CFL condition, the stability of the scheme under the form:

$$0 \leq C_k^{i,n} \leq M, \quad \forall k \in [1, N], \quad \forall n \in [0, \infty[, \quad i = 1, 2, 3. \tag{52}$$

First step. Existence of a family of discrete supersolutions. We build a nonnegative vector $U = (U_1^1, \dots, U_N^1, U_1^2, \dots, U_N^2, U_1^3, \dots, U_N^3)$ such that

$$\left\{ \begin{array}{l} U_k^1 - U_{k-1}^1 \geq \frac{\Delta x}{3} \left[U_k^2 + U_k^3 - 2U_k^1 + V_m \frac{U_k^3}{1+U_k^3} \right], \quad k \in [1, N], \\ U_k^2 - U_{k-1}^2 \geq \frac{\Delta x}{3} \left[U_k^1 + U_k^3 - 2U_k^2 + V_m \frac{U_k^3}{1+U_k^3} \right], \quad k \in [1, N], \\ U_{k+1}^3 - U_k^3 \geq \frac{\Delta x}{3} \left[U_k^1 + U_k^2 - 2U_k^3 - 2V_m \frac{U_k^3}{1+U_k^3} \right], \quad k \in [1, N], \\ U_0^1 > C_0^1, \quad U_0^2 > C_0^2, \quad U_{N+1}^3 = U_N^2, \end{array} \right. \tag{53}$$

and

$$U_k^i \geq C_k^{i,0}, \quad \forall k \in [1, N], \quad i = 1, 2, 3, \tag{54}$$

We define the matrix $A = A_{\Delta x}$ such that solving 53 is equivalent to finding U which satisfies

$$AU \geq 0, \tag{55}$$

where a matrix $M \geq 0$ if all its elements are nonnegative.

A is irreducible [18], and

$$\exists j_0 \text{ such as } a_{j_0, j_0} - \sum_{\substack{1 \leq i \leq 3N \\ i \neq j_0}} a_{i, j_0} > 0, \quad (j_0 = 2N + 1)$$

Using the M-matrix theory, A is invertible and A^{-1} is positive (that is to say all its coefficients are positive). We then choose $x > 0$, $x \in \mathbb{R}^{3N}$. We have $A^{-1}x = y > 0$, so $Ay = x$. We can choose α such that

$$\alpha y \geq C^0, \quad \alpha y_1 \geq C_0^1, \quad \alpha y_{N+1} \geq C_0^2. \tag{56}$$

Thus, $U = \alpha y$ satisfies 53 and 54.

Second step. The induction. Assuming that for a given n

$$C_k^{i,n} \leq U_k^i \quad \forall k \in [1, N] \quad i = 1, 2, 3. \tag{57}$$

Then,

$$\begin{aligned} C_k^{1,n+1} &= \left[1 - \frac{2}{3}\Delta t - \frac{\Delta t}{\Delta x} \right] C_k^{1,n} + \frac{\Delta t}{\Delta x} C_{k-1}^{1,n} + \frac{\Delta t}{3} C_k^{2,n} + \frac{\Delta t}{3} C_k^{3,n} + V_m \frac{\Delta t}{3} \frac{C_k^{3,n}}{1+C_k^{3,n}}, \\ &\leq \left[1 - \frac{2}{3}\Delta t - \frac{\Delta t}{\Delta x} \right] U_k^{1,n} + \frac{\Delta t}{\Delta x} U_{k-1}^{1,n} + \frac{\Delta t}{3} U_k^{2,n} + \frac{\Delta t}{3} U_k^{3,n} + V_m \frac{\Delta t}{3} \frac{U_k^{3,n}}{1+U_k^{3,n}}, \\ &\leq U_k^1. \end{aligned}$$

The same calculation holds for $C_k^{2,n+1}$ and $C_k^{3,n+1}$. Since 54 holds true, we deduce 52 with $M = \max \{U_k^i, k \in [1, N], i = 1, 2, 3\}$.

4.2. Steady states. We then use this method to compute a numerical solution to 7, iterating the scheme for n large enough with the initial data $C^j(x, 0) = 1$ for $j = 1, 2$ and 3.

Figure 2 depicts the concentration profiles at steady state for different values of V_m . We observe that if V_m is large enough, there is a longitudinal gradient of concentration, as observed physiologically.

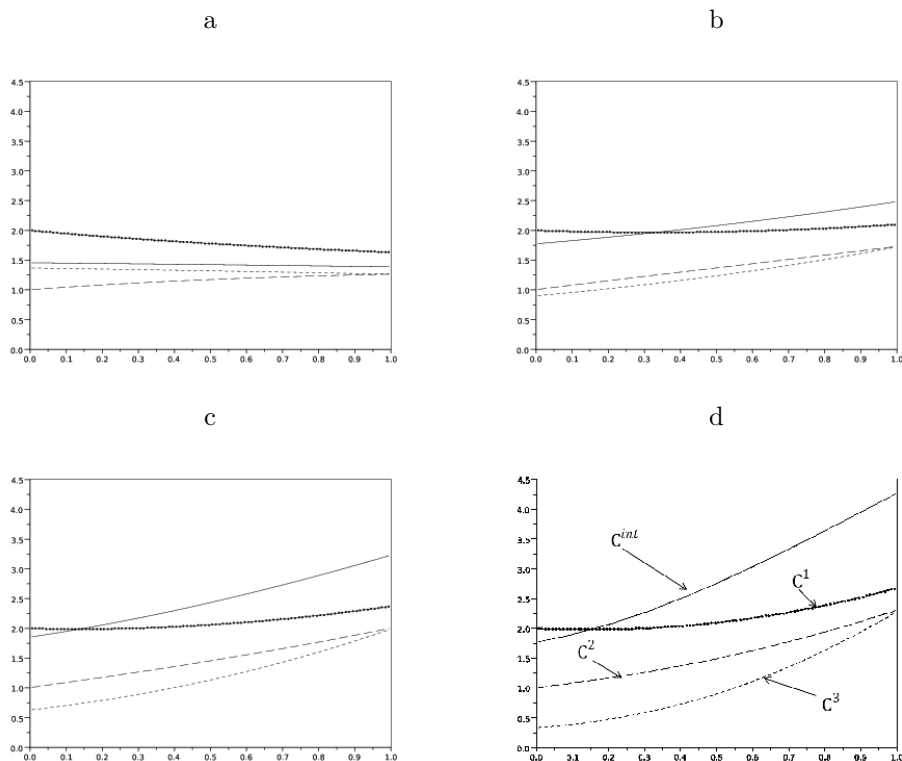


FIGURE 2. Concentration profiles at steady state in different tubes, along the x -axis. The thin solid curve represents C^{int} , the thick curve C^1 , the dashed curve C^2 , and the dotted curve C^3 . Parameters: $C_0^1 = 2$ and $C_0^2 = 1$, $L = 1$, $\Delta x = 0.01$, $Nc = 0.99$, where $Nc = \frac{\Delta t}{\Delta x}$. The pump velocity V_m is taken as 0 (a), 3 (b), 5 (c), and 8 (d). The profiles are obtained after 1000 time iterations.

In order to assert the exponential convergence of the algorithm (as predicted by the theory), we define for each time step n the indicator

$$c(n) = \max_{k \in [1, N]} \|C_k^n - C_k^{n-1}\|_\infty.$$

Displayed in Figure 3 is the plot of $\log(c(n))$ as a function of the number of time iterations n . Our results indicate that the exponential convergence holds true even for large values of V_m , even though the decay rate is then slower. A physiological

interpretation could be that the higher V_m , the more significant the concentration gradient, and the longer the time needed to reach equilibrium.

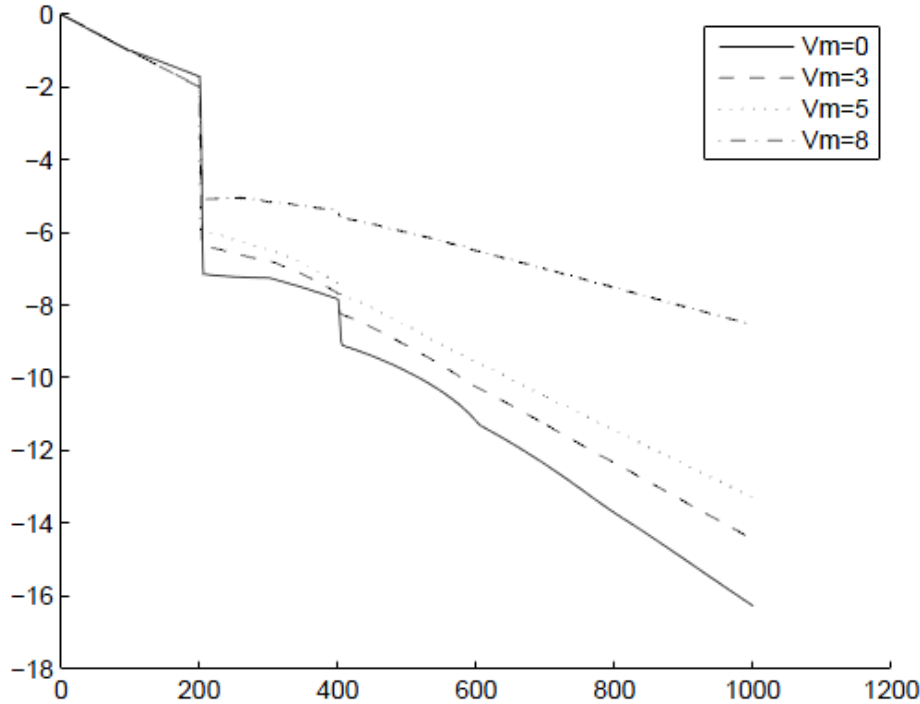


FIGURE 3. Log-convergence of the dynamic problem toward the steady state solution, for different values of V_m . The x -axis represents n , the number of time iterations, and the y -axis represents $\log(c(n))$. The parameters are the same as those used in Figure 2. The convergence slows down as V_m increases.

4.3. **The linear case $V_m = 0$.** If we ignore active transport, the system becomes linear. In this case we prove that the convergence toward the equilibrium state is of order $e^{-\lambda t}$ with λ the first eigenvalue as described in Appendix C.

For different values of L , on one hand, we calculate the eigenvalue λ in 69 using the power algorithm, and on the other hand, we compute the logarithmic rate of convergence for the numerical solution to 8 as t grows. The theoretical and numerical values are compared in Table 2.

5. **Countercurrent exchange across 2 tubes.** The counter-current arrangement of tubules and vessels in the kidney has long been known to improve the production of concentrated urine (for a review, see [19]). The concentrating capacity of the kidney is reflected by the increase in fluid osmolality (or concentration) along the collecting duct and can therefore be quantified by the interstitial axial concentration gradient. In order to assess the extent to which the counter-arrangement architecture enhances concentration gradients, we then consider a simpler system

TABLE 2. Comparison between the first eigenvalue λ of the differential operator 69 and the value γ of the numerical gradient of the logarithmic convergence, for different tube lengths (L). The two values are obtained as described in the text in the linear case $V_m = 0$.

L	0.1	0.5	1	2	3	6
λ	25.530	3.299	1.3044	0.509	0.296	0.125
γ	25.166	3.234	1.3044	0.517	0.292	0.109

consisting of two tubes only. Note first that if there were no pump (i.e., no active transport of solute out of one the tubes), the concentration of solute would remain constant, independent of x , in both tubes (results not shown). In other words, the pump creates a transversal concentration gradient (referred to as the “single effect”), which in turn generates an axial osmolality gradient [20], [19]. The multiplication of the single effect in the axial direction concentrates the fluid flowing downwards. Our simple 2-tubule model illustrates why multiplication of the single effect is greater in counter-current flows than in cocurrent flows.

5.1. Countercurrent versus cocurrent exchange. Garner et al. [5] undertook a similar study, in which they solved analytically the time-dependent linear system relative to 58, using a Laplace transform which was numerically inverted. In this study, we solve analytically 58 and 59 to compare the steady state solutions of a countercurrent and a cocurrent architecture, assuming a linear rate for the pump. We then solve numerically the corresponding dynamic system using the finite volume scheme. The advantages of our numerical method are that it can be extended to n tubes ($n \geq 2$), and that we could assume a nonlinear term for active transport.

Countercurrent flows. When the tubes are arranged in a counter-current manner, the conservation equations can be written as

$$\begin{cases} \frac{dC^1(x)}{dx} = J^1(x), & -\frac{dC^2(x)}{dx} = J^2(x), & x \in [0, L], \\ C^1(0) = C_0^1, & C^2(L) = C^1(L). \end{cases} \quad (58)$$

The fluxes are given by

$$J^1(x) = C^{int}(x) - C^1(x), \quad J^2(x) = C^{int}(x) - C^2(x) - V_m C^2(x).$$

with the condition

$$J^1 + J^2 = 0.$$

We infer from this condition that

$$C^{int}(x) = \frac{1}{2} [C^1(x) + C^2(x) + V_m C^2(x)], \quad C^1(x) - C^2(x) = \text{constant}.$$

Knowing that $C^1(L) = C^2(L)$, we conclude that $C^1 = C^2$. Then the system reduces to a single equation

$$\begin{cases} \frac{dC^1(x)}{dx} = \frac{1}{2} V_m C^1(x), & C^1(0) = C_0^1. \\ C^2(x) = C^1(x). \end{cases}$$

We can calculate the analytical solution

$$C^1(x) = C_0^1 e^{\frac{V_m}{2}x}.$$

Cocurrent flows. In a cocurrent architecture, the equations are

$$\begin{cases} \frac{dC^3(x)}{dx} = J^3(x), & \frac{dC^4(x)}{dx} = J^4(x), \\ C^3(0) = C_0 = C^4(0). \end{cases} \quad (59)$$

The fluxes are still given by

$$J^3(x) = C^{int}(x) - C^3(x), \quad J^4(x) = C^{int}(x) - C^4(x) - V_m C^4(x).$$

With similar arguments, we obtain the solution

$$\begin{cases} C^3(x) = 2C_0 \left[\frac{1 + V_m}{2 + V_m} - \frac{V_m}{2(2 + V_m)} e^{(-1 - \frac{V_m}{2})x} \right], \\ C^4(x) = 2C_0 \left[\frac{1}{2 + V_m} + \frac{V_m}{2(2 + V_m)} e^{(-1 - \frac{V_m}{2})x} \right]. \end{cases}$$

In both configurations, there is a gradient of concentration in the descending tubes (tubes 1 and 3). In the countercurrent configuration, the gradient is exponential in both tubes, with parameter $\frac{V_m}{2}$, where V_m quantifies the single-effect. In the cocurrent configuration, the gradient is lower, and in the best case (L and V_m very large), $C^3(L)$ tends toward $2C_0$ whereas $C^4(L)$ falls near 0.

Shown in figure 4 are concentration profiles solution to 58 and 59.

5.2. Visualization of the dynamic of a countercurrent-flows system relaxing toward the steady state. To visualize the evolution of concentration profiles with time, we consider the dynamic problem with countercurrent flows, assuming as the initial condition that the concentration is equal to C_0 all along the tubes. We display some curves of concentration profiles at different times and see them evolve toward the equilibrium state. We introduce the equation describing this dynamic problem

$$\begin{cases} \frac{\partial C^1}{\partial t}(x, t) + \frac{\partial C^1}{\partial x}(x, t) = J^1(x, t), & x \in [0, L], t > 0, \\ \frac{\partial C^2}{\partial t}(x, t) - \frac{\partial C^2}{\partial x}(x, t) = J^2(x, t), & x \in [0, L], t > 0, \\ C^1(0, t) = C_0^1, \quad C^2(L, t) = C^1(L, t). \end{cases} \quad (60)$$

which we complete with nonnegative initial concentrations $C^1(x, 0), C^2(x, 0)$. The fluxes are given by:

$$\begin{aligned} J^1(x, t) &= C^{int}(x, t) - C^1(x, t), \\ J^2(x, t) &= C^{int}(x, t) - C^2(x, t) - V_m C^2(x, t), \end{aligned}$$

with the condition:

$$J^1(x, t) + J^2(x, t) = 0.$$

Shown in Figure 5 are concentration profiles at different times in 2 tubes arranged in a counter-current manner, with a pump in the ascending tube, solution to 60 obtained using a finite volume scheme.

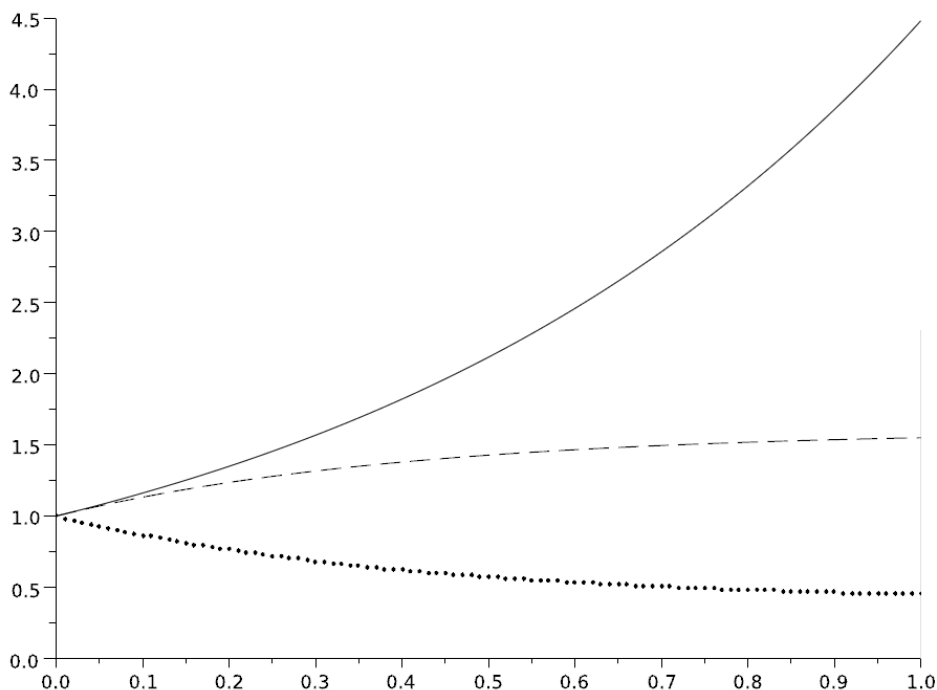


FIGURE 4. The solid curve represents the steady state concentration profile ($C^1 = C^2$) for the countercurrent arrangement. The dashed curve (C^3) and the dotted curve (C^4) represent steady state concentration profiles in the cocurrent arrangement. The pump term is taken to be linear here.

6. Conclusion and perspectives. Using a simplified model of solute exchange across 3 kidney tubules, all of which were taken to be water impermeable, we demonstrated the existence and uniqueness of the stationary state. In addition, we showed that the dynamic solution converges toward the steady state solution, and that the convergence is exponential if the maximum rate of the pump mediating active transport in one of the tubes is not too high. Finally, our results illustrate how the counter-current arrangement of tubules enhances the axial concentration gradient, thereby favoring the production of highly concentrated urine.

Under physiological conditions, water and solute flows are tightly coupled in the kidney: osmosis (i.e., transmembrane concentration gradients) is the main driving force for water exchange, and solute movement is partly driven by convection. Hence, the system of nonlinear differential equations yielding solute and water flows must generally be solved numerically. In this study, we chose to make some simplifying assumptions (such as that of water-impermeable tubules) in order to better characterize this system of differential equations, and to determine the existence and uniqueness of the solution. To the best of our knowledge, there have been few previous attempts to do so in comparable systems [12, 6]. Layton [12] showed that for sufficiently low or sufficiently large rates of NaCl active transport, there exists a unique solution to the Peskin model[11]. The latter model also considers three tubules surrounded by a common interstitium, but it differs significantly from

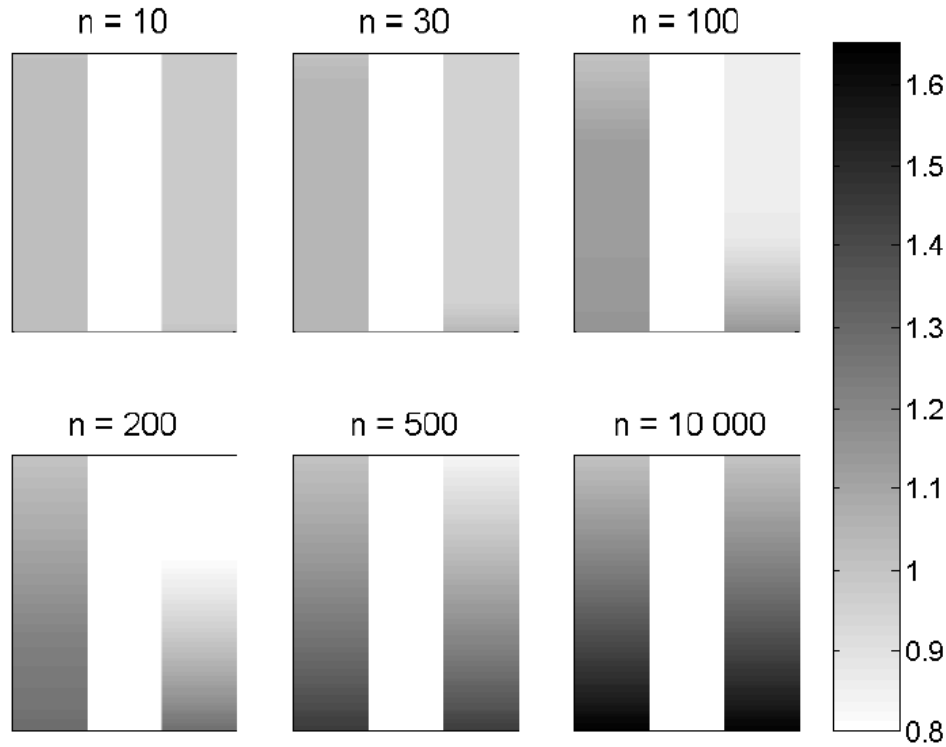


FIGURE 5. Concentration profiles at different time iterations n in 2 tubes arranged in a countercurrent manner, with a pump in the ascending one. The pump rate is taken to increase linearly with the concentration C , see 60. Parameters: $L = 1$, $C^0 = 1$, $V_m = 1$, $\Delta x = 0.01$, $\Delta t = 0.0099$.

ours in that it assumes that solute concentration is equal in the descending limb (i.e., tube 2 in our representation), the collecting duct (i.e., tube 1), and the interstitium at each level. For the model considered in the present study, we showed that the steady state solution exists and is unique for any given value of V_m (i.e., the maximum rate of NaCl active transport out of the ascending limb). We also demonstrated that the solution to the dynamic model always converges toward the steady state solution. Moreover, if V_m is small enough, namely if condition (13) is satisfied, then the convergence is exponential with time.

It was recognized early on, as reviewed by Stephenson ([19]), that the formation of a large axial concentration gradient in the kidney is made possible by the fact that tubules (1) exhibit differential permeabilities and (2) are arranged in a counterflow manner. To assess the degree to which the counter-current architecture increases the axial concentration gradient, relative to the cocurrent configuration, we used a 2 tube system and derived an analytical solution for solute concentration profiles. Our results suggest that solute concentration increases exponentially with x in the former case (with an exponential factor that is proportional to V_m), whereas it is bounded independently of V_m in the latter case.

A similar exponential concentration increase was predicted for the single loop cycling model with constant water flows [5]. The investigators used Laplace transforms to obtain numerical solutions for two limiting cases: when the pump is either saturated (i.e., the active transport rate is a constant) or very far from saturation (i.e., the rate is a linear function of concentration). Their study cannot be easily extended to account for nonlinear rates, and for more than two tubes, as calculations would then become impracticable. In contrast, the method we developed could be extended to consider more tubules, and could apply to nonlinear rates.

A more realistic representation of kidney function would require accounting for transversal water movement. Whether the existence and uniqueness of steady state solutions to such problems can then be proven remains to be determined.

Acknowledgments. Funding for this study was provided by the program EMERGENCE (EME 0918) of the Université Pierre et Marie Curie (Paris Univ. 6). We would also like to thank Dr. S. R. Randall for helpful discussions.

Appendix A. Definition of weak solutions. A weak solution to 8 is a function $C \in C([0, T], L^1[0, L])^3$ such that for all $\Phi \in V$ defined in 32, we have

$$\begin{aligned}
& \int_0^T \int_0^L \frac{\partial \Phi}{\partial t} \cdot C(x, t) dx dt + \int_0^T \int_0^L \frac{\partial \Phi}{\partial x} \cdot (C^1, C^2, -C^3)(x, t) dx dt \\
&= \frac{2}{3} \int_0^T \int_0^L \Phi \cdot C(x, t) dx dt + \frac{2}{3} \int_0^T \int_0^L \Phi^3 F(C^3, x)(x, t) dx dt \\
&\quad - \frac{1}{3} \int_0^T \int_0^L [\Phi^1 (C^2 + C^3 + F(C^3, x))(x, t)] dx dt \\
&\quad - \frac{1}{3} \int_0^T \int_0^L [\Phi^2 (C^1 + C^3 + F(C^3, x))(x, t)] dx dt \tag{61} \\
&\quad - \frac{1}{3} \int_0^T \int_0^L [\Phi^3 (C^1 + C^2)(x, t)] dx dt \\
&\quad + \int_0^T \Phi^1(0, t) C^1(0, t) dt + \int_0^T \Phi^2(0, t) C^2(0, t) dt \\
&\quad + \int_0^L \Phi(x, T) \cdot C(x, T) dx - \int_0^L \Phi(x, 0) \cdot C(x, 0) dx.
\end{aligned}$$

For 7, the definition of a weak solution $C \in (L^1[0, L])^3$ uses test functions $\Phi \in W$ with

$$W = \{\Phi \in (C^1([0, L]))^3, \quad \Phi^1(L) = \Phi^3(0) = 0, \quad \Phi^3(L) = \Phi^2(L)\},$$

and is written

$$\begin{aligned}
& \int_0^L \frac{d\Phi}{dx} \cdot (C^1, C^2, -C^3)(x) dx = \frac{2}{3} \int_0^L \Phi \cdot C(x, t) dx + \frac{2}{3} \int_0^L \Phi^3 F(C^3, x)(x) dx \\
& - \frac{1}{3} \int_0^L [\Phi^1 (C^2 + C^3 + F(C^3, x))(x)] dx - \frac{1}{3} \int_0^L [\Phi^2 (C^1 + C^3 + F(C^3, x))(x)] dx \\
& \quad - \frac{1}{3} \int_0^L [\Phi^3 (C^1 + C^2)(x)] dx - \Phi^1(0) C^1(0) - \Phi^2(0) C^2(0).
\end{aligned}$$

Appendix B. Existence of a solution to 42. In subsection 3.5, we have used the fact that there are nonnegative solutions to

$$\begin{cases} \frac{dC^1(x)}{dx} + \frac{2}{3}C^1(x) = \frac{1}{3} [C^2(x) + C^3(x) + F(C^3(x), x)], \\ \frac{dC^2(x)}{dx} + \frac{2}{3}C^2(x) = \frac{1}{3} [C^1(x) + C^3(x) + F(C^3(x), x)], \\ -\frac{dC^3(x)}{dx} + \frac{2}{3} [C^3(x) + F(C^3(x), x)] = \frac{1}{3} [C^1(x) + C^2(x)], \\ C^1(0) = C_0^1 > 0, \quad C^2(0) = C_0^2 > 0, \quad C^3(L) = C_L^3 \geq 0. \end{cases} \quad (62)$$

and that they are monotonic with respect to the boundary values. We prove these statements here.

First step. A regularized problem. For every $\alpha > 0$, we prove that the following system has a solution C which is nonnegative

$$\begin{cases} \frac{dC^1(x)}{dx} + \frac{2}{3}C^1(x) + \alpha C^1(x) = \frac{1}{3} [C^2(x) + C^3(x) + F(C^3(x), x)], \\ \frac{dC^2(x)}{dx} + \frac{2}{3}C^2(x) + \alpha C^2(x) = \frac{1}{3} [C^1(x) + C^3(x) + F(C^3(x), x)], \\ -\frac{dC^3(x)}{dx} + \frac{2}{3} [C^3(x) + F(C^3(x), x)] = \frac{1}{3} [C^1(x) + C^2(x)], \\ C^1(0) = C_0^1 > 0, \quad C^2(0) = C_0^2 > 0, \quad C^3(L) = C_L^3 \geq 0. \end{cases} \quad (63)$$

To do so, we use the Banach-Picard theorem in the Banach space

$$X = L^1([0, L], \mathbb{R}^+) \times L^1([0, L], \mathbb{R}^+), \quad \|(C^1, C^2)\|_X = \int_0^L (C^1(x) + C^2(x)) dx.$$

For $(D^1, D^2) \in X$, we define (C^1, C^2) the solution to

$$\begin{cases} \frac{dC^1(x)}{dx} + \frac{2}{3}C^1(x) + \alpha C^1(x) = \frac{1}{3} [D^2(x) + C^3(x) + F(C^3(x), x)], \\ \frac{dC^2(x)}{dx} + \frac{2}{3}C^2(x) + \alpha C^2(x) = \frac{1}{3} [D^1(x) + C^3(x) + F(C^3(x), x)], \\ -\frac{dC^3(x)}{dx} + \frac{2}{3} [C^3(x) + F(C^3(x), x)] = \frac{1}{3} [D^1(x) + D^2(x)], \\ C^1(0) = C_0^1 > 0, \quad C^2(0) = C_0^2 > 0, \quad C^3(L) = C_L^3 \geq 0. \end{cases} \quad (64)$$

Then, we claim that the operator

$$\mathcal{B} : (D^1, D^2) \mapsto (C^1, C^2) := \mathcal{B}(D^1, D^2)$$

has a unique fixed point in X_+ (the cone of nonnegative functions), which follows from the two properties

$$(a) \mathcal{B} : X_+ \longrightarrow X_+, \quad (b) \mathcal{B} \text{ is a strong contraction.}$$

Second step. The fixed point. To prove (a), we check that (C^1, C^2) are nonnegative functions. The Cauchy Lipschitz theorem tells us that there is a unique C^3 , which is a nonnegative continuous solution to the third equation of 64 (here we use assumption 9). Then, we again apply the Cauchy Lipschitz theorem to the first two equations of 64 to obtain that C^1 and C^2 are continuous and positive functions.

Now, we check (b). By substractions of solutions, say (C^1, C^2) and $(\overline{C^1}, \overline{C^2})$ for two different D , say (D^1, D^2) and $(\overline{D^1}, \overline{D^2})$, we obtain

$$\left\{ \begin{array}{l} \frac{d(C^1 - \overline{C^1})}{dx}(x) + (\frac{2}{3} + \alpha)(C^1 - \overline{C^1}) \\ \qquad \qquad \qquad = \frac{1}{3}[(D^2 - \overline{D^2})(x) + (C^3 - \overline{C^3})(x) + F(C^3(x), x) - F(\overline{C^3}(x), x)], \\ \frac{d(C^2 - \overline{C^2})}{dx}(x) + (\frac{2}{3} + \alpha)(C^2 - \overline{C^2}) \\ \qquad \qquad \qquad = \frac{1}{3}[(D^1 - \overline{D^1})(x) + (C^3 - \overline{C^3})(x) + F(C^3(x), x) - F(\overline{C^3}(x), x)], \\ -\frac{d(C^3 - \overline{C^3})}{dx}(x) + \frac{2}{3}[(C^3 - \overline{C^3})(x) + F(C^3(x), x) - F(\overline{C^3}(x), x)] \\ \qquad \qquad \qquad = \frac{1}{3}[(D^1 - \overline{D^1})(x) + (D^2 - \overline{D^2})(x)], \\ (C^1 - \overline{C^1})(0) = 0, \quad (C^2 - \overline{C^2})(0) = 0, \quad (C^3 - \overline{C^3})(L) = 0. \end{array} \right.$$

We use the notations

$$\delta^i(x) := (C^i(x) - \overline{C^i}(x)), \quad i = 1, 2, 3,$$

$$G(x) = F(C^3(x), x) - F(\overline{C^3}(x), x).$$

As in subsection 3.3 and using the same notations, we obtain the following inequalities

$$\left\{ \begin{array}{l} \frac{d|\delta^1|}{dx} + (\frac{2}{3} + \alpha)|\delta^1| = \frac{1}{3} \text{sign}(\delta^1)(D^2 - \overline{D^2} + \delta^3 + F(C^3) - F(\overline{C^3})), \\ \frac{d|\delta^2|}{dx} + (\frac{2}{3} + \alpha)|\delta^2| = \frac{1}{3} \text{sign}(\delta^2)(D^1 - \overline{D^1} + \delta^3 + F(C^3) - F(\overline{C^3})), \\ -\frac{d|\delta^3|}{dx} + \frac{2}{3}(|\delta^3| + G) = \frac{1}{3} \text{sign}(\delta^3)(D^1 - \overline{D^1} + D^2 - \overline{D^2}). \end{array} \right. \quad (65)$$

Integrating these inequalities, we conclude that

$$\begin{aligned} & |\delta^1(L)| + |\delta^2(L)| + |\delta^3(0)| + \int_0^L (\alpha + \frac{2}{3})|\delta^1| + \int_0^L (\alpha + \frac{2}{3})|\delta^2| \\ & \quad + \frac{1}{3} \int_0^L [2 \text{sign}(\delta^3) - \text{sign}(\delta^1) - \text{sign}(\delta^2)](\delta^3 + F(C^3) - F(\overline{C^3})) \\ & = \frac{1}{3} \int_0^L [\text{sign}(\delta^2) + \text{sign}(\delta^3)](D^1 - \overline{D^1}) + \frac{1}{3} \int_0^L [\text{sign}(\delta^1) + \text{sign}(\delta^3)](D^2 - \overline{D^2}), \end{aligned}$$

which gives us

$$\int_0^L (\alpha + \frac{2}{3})(|\delta^1| + |\delta^2|) \leq \frac{2}{3} \int_0^L [|D^1 - \overline{D^1}| + |D^2 - \overline{D^2}|]. \quad (66)$$

In terms of the Banach space under consideration, this is to say

$$\|(C^1, C^2) - (\overline{C^1}, \overline{C^2})\|_X \leq \frac{2}{2 + 3\alpha} \|(D^1, D^2) - (\overline{D^1}, \overline{D^2})\|_X,$$

and we obtain the strong contraction property, and thus the existence of a solution to 63.

Third step. The limit $\alpha = 0$. From now on, we denote the solution to 63 as $C_\alpha = (C_\alpha^1, C_\alpha^2, C_\alpha^3)$; it is Lipschitz continuous because F is. We prove here that the family $(C_\alpha)_{\alpha>0}$ is equicontinuous on $[0, L]$. Then we may apply the Ascoli theorem to obtain a strongly convergent subsequence and conclude the proof.

From 63, we deduce that

$$\frac{d}{dx}(C_\alpha^1(x) + C_\alpha^2(x) - C_\alpha^3(x)) \leq 0, \tag{67}$$

which tells us that

$$C_\alpha^1(L) + C_\alpha^2(L) + C_\alpha^3(0) \leq C_\alpha^1(0) + C_\alpha^2(0) + C_\alpha^3(L) = C_0^1 + C_0^2 + C_L^3.$$

We deduce that $C_\alpha^1(L), C_\alpha^2(L)$ and $C_\alpha^3(0)$ are uniformly bounded in α . Then, using the fact that the endpoints are controlled, 67 tells us that the function h defined as

$$h(x) = C_\alpha^1(x) + C_\alpha^2(x) - C_\alpha^3(x) \tag{68}$$

is uniformly bounded in α too. Inserting this in the third line of 63, we write

$$-\frac{d}{dx}C_\alpha^3 + \frac{2}{3}(C_\alpha^3 + F(C_\alpha^3)) = \frac{C_\alpha^3 + h}{3},$$

so that C_α^3 is uniformly bounded in α . Using the first and second lines of 63, we also conclude that $(C_\alpha^1 + C_\alpha^2)$ are uniformly bounded in α , and so are C_α^1 and C_α^2 .

Fourth step. The comparison principle. As it was done in the Second step, and using again the argument of subsection 3.3 (replacing the absolute value by the positive part), one obtains that if $C_0^1 \geq \bar{C}_0^1$, $C_0^2 \geq \bar{C}_0^2$ and $C_L^3 \geq \bar{C}_L^3$, then $C^i(x) \geq \bar{C}^i(x)$ for all $x \in [0, L]$ and $i = 1, 2$ and 3 .

Appendix C. Existence of eigenelements. As often in nonlinear problems, the eigenelements for the linear problem play an important role in the understanding of nonlinear effects. We state the first eigenelement problem and recall some properties here. For a given continuous function $\mu(x) > 0$, this consists in finding $(\Lambda(\mu), N(x; \mu) \geq 0, \phi(x, \mu) \geq 0)$ solutions to the direct and dual problems defined as

$$\left\{ \begin{array}{l} \frac{dN^1(x)}{dx} = \frac{1}{3}[N^2(x) + (1 + \mu(x))N^3(x)] + (\Lambda - \frac{2}{3})N^1, \\ \frac{dN^2(x)}{dx} = \frac{1}{3}[N^1(x) + (1 + \mu(x))N^3(x)] + (\Lambda - \frac{2}{3})N^2, \\ -\frac{dN^3(x)}{dx} = \frac{1}{3}[N^1(x) + N^2(x)] + (\Lambda - \frac{2}{3}(1 + \mu(x)))N^3, \\ N^1(0) = 0, \quad N^2(0) = 0, \quad N^3(L) = N^2(L). \end{array} \right. \tag{69}$$

$$\left\{ \begin{array}{l} -\frac{d\phi^1(x)}{dx} = \frac{1}{3}[\phi^2(x) + \phi^3(x)] + (\Lambda - \frac{2}{3})\phi^1, \\ -\frac{d\phi^2(x)}{dx} = \frac{1}{3}[\phi^1(x) + \phi^3(x)] + (\Lambda - \frac{2}{3})\phi^2, \\ \frac{d\phi^3(x)}{dx} = \frac{1 + \mu(x)}{3}[\phi^1(x) + \phi^2(x)] + (\Lambda - \frac{2}{3}(1 + \mu(x)))\phi^3, \\ \phi^1(L) = 0, \quad \phi^3(0) = 0, \quad \phi^2(L) = \phi^3(L). \end{array} \right. \tag{70}$$

It is also standard to normalize the eigenfunctions as

$$\int_0^L (N^1 + N^2 + N^3) = 1, \quad \int_0^L (N^1\phi^1 + N^2\phi^2 + N^3\phi^3) = 1. \tag{71}$$

Finally we use the notation $k(\mu)$:

$$k := k(\mu) \text{ is the biggest real number such that } \phi^1 + \phi^2 \geq k\phi^3. \quad (72)$$

The standard result *à la* Krein-Rutman is

Proposition 1. *For $\mu > 0$ there is a (smooth) solution with $\Lambda(\mu) > 0$. Moreover we have: $N^1(x) > 0$, $N^2(x) > 0$ for $x > 0$, $N^3 > 0$ and $\phi^1(x) > 0$ for $x < L$, $\phi^3(x) > 0$ for $x > 0$, $\phi^2 > 0$.*

Strategy for the proof. We consider the implicit scheme with space step h associated with 69. We call A_h the matrix of the scheme. We can prove that A_h is invertible and that its inverse is positive. Thus, the Perron Frobenius theorem yields the existence of $\lambda_h > 0$, $N_h \geq 0$, $\phi_h \geq 0$, solution to the eigenproblem

$$A_h N_h = \lambda_h N_h, \quad {}^t A_h \phi_h = \lambda_h \phi_h.$$

Since $(\lambda_h)_h$ is bounded by $1 + \text{spec}(A)$, there is a subsequence (λ_h) such that

$$\lim_{h \rightarrow 0} \lambda_h = \lambda > 0.$$

From the discrete functions N_h and ϕ_h we build, as in section 3, continuous piecewise functions. Applying the Ascoli theorem to the bounded and equicontinuous families $(N_h)_h$ and $(\phi_h)_h$, we also prove that there are subsequences (λ_h) , (ϕ_h) such as

$$\lim_{h \rightarrow 0} N_h = N \geq 0, \quad \lim_{h \rightarrow 0} \phi_h = \phi \geq 0,$$

with N and ϕ satisfying the condition 71. Then, we prove that λ, N, ϕ satisfy 69, 70.

Proof of the exponential convergence. We define, with the notation of section 2.2

$$M(t) = \int_0^L \left[d^1(x, t) \phi_1(x) + d^2(x, t) \phi_2(x) + d^3(x, t) \phi_3(x) \right] dx.$$

The usual duality argument (see [17]) gives, with G defined in section 3.3

$$\begin{aligned} \frac{d}{dt} M(t) &\leq -\lambda M(t) + \frac{1}{3} \int_0^L (G - \mu(x) d^3) (\phi_1(x) + \phi_2(x) - 2\phi_3(x)) dx \\ &\leq -\lambda M(t) + \frac{(k-2)}{3} \int_0^L (G - \mu(x) d^3) \phi_3(x) dx \end{aligned}$$

because $G \leq \mu(x) d^3$.

If, in 72, $k(\mu) \geq 2$, the result follows from the Gronwall lemma.

Otherwise $k - 2 < 0$ and we write, treating only the case $C^3 \leq \overline{C^3}$ to simplify

$$(2-k)[\mu(x)d^3 - G] = \int_{C^3}^{\overline{C^3}} [\mu(x) - F_C(c, x)] dc \leq d^3[\Lambda - \delta]$$

with $\delta > 0$ given by the difference between the right and left hand sides in 17. From this we conclude that

$$\frac{d}{dt} M(t) \leq -\delta M(t)$$

and the exponential convergence again follows from the Gronwall lemma. \square

REFERENCES

- [1] G. Allaire, “Numerical Analysis and Optimization,” Numerical Mathematics and Scientific Computation. Oxford University Press, Oxford, 2007. An introduction to mathematical modelling and numerical simulation, Translated from the French by Alan Craig.
- [2] F. Bouchut, “Non Linear Stability of Finite Volume Methods for Hyperbolic Conservation Laws and Well Balanced Schemes for Sources,” Birkhäuser-Verlag, 2004.
- [3] C. M. Dafermos, “Hyperbolic Conservation Laws in Continuum Physics,” **325** of Grundlehren der Mathematischen Wissenschaften [Fundamental Principles of Mathematical Sciences]. Springer-Verlag, Berlin, third edition, 2010.
- [4] L. C. Evans, “Partial Differential Equations,” **19** of Graduate Studies in Mathematics, American Mathematical Society, Providence, RI, second edition, 2010.
- [5] J. Garner, K. Crump and J. Stephenson, *Transient behaviour of the single loop solute cycling model of the renal medulla*, Bulletin of Mathematical Biology, **40** (1978), 273–300.
- [6] J. B. Garner and R. B. Kellogg, *Existence and uniqueness of solutions in general multisolute renal flow problems*, Journal of Mathematical Biology, **26** (1988), 455–464.
- [7] E. Godlewski and P. A. Raviart, “Numerical Approximation of Hyperbolic Systems of Conservation Laws,” **118** of Applied Mathematical Sciences, Springer-Verlag, New York, 1996.
- [8] M. A. Katsoulakis and A. E. Tzavaras, *Contractive relaxation systems and the scalar multidimensional conservation law*, Comm. Partial Differential Equations, **22** (1997), 195–233.
- [9] A. T. Layton and H. E. Layton, *A semi-Lagrangian semi-implicit numerical method for models of the urine concentrating mechanism*, SIAM Journal on Scientific Computing, **23** (2002), 1526–1548.
- [10] H. Layton and E. Pitman, *A dynamic numerical method for models of renal tubules*, Bulletin of Mathematical Biology, **56** (1994), 547–565.
- [11] H. E. Layton, *Distribution of henle’s loops may enhance urine concentrating capability*, Biophysical Journal, **49** (1986), 1033–1040.
- [12] H. E. Layton, *Existence and uniqueness of solutions to a mathematical model of the urine concentrating mechanism*, Mathematical Biosciences, **84** (1987), 197–210.
- [13] H. E. Layton, E. Bruce Pitman and Mark A. Knepper, *A dynamic numerical method for models of the urine concentrating mechanism*, SIAM J. Appl. Math., **55** (1995), 1390–1418.
- [14] R. J. LeVeque, “Finite Volume Methods for Hyperbolic Problems,” Cambridge University Press, 2002.
- [15] L. C. Moore and D. J. Marsh, *How descending limb of Henle’s loop permeability affects hypertonic urine formation*, Am J Physiol Renal Physiol, **239** (1980), F57–71.
- [16] R. Natalini, *Convergence to equilibrium for the relaxation approximations of conservation laws*, Communications on Pure and Applied Mathematics, **49** (1996), 795–823.
- [17] B. Perthame, “Transport Equations in Biology,” Frontiers in Mathematics. Birkhäuser Verlag, Basel, 2007.
- [18] D. Serre, “Matrices,” **216** of Graduate Texts in Mathematics. Springer, New York, second edition, 2010. Theory and applications.
- [19] J. L. Stephenson, “Urinary Concentration and Dilution: Models,” Oxford University Press, New-York, 1992.
- [20] K. Werner and B. Hargitay, *The multiplication principle as the basis for concentrating urine in the kidney (with comments by Bart Hargitay and S. Randall Thomas)*, J. Am. Soc. Nephrol., **12** (2001), 1566–1586.

Received September 2011; revised October 2012.

E-mail address: magali.tournus@ann.jussieu.fr

E-mail address: aurelie.edwards@crc.jussieu.fr

E-mail address: nicolas.seguin@upmc.fr

E-mail address: benoit.perthame@upmc.fr